

OPTRA

June 17, 1998

Commander
U.S. Army Aviation and Missile Command
ATTN: AMSAM-RD-WS-DP-SB/Mr. Johnson
Building 7804, Room 207
Redstone Arsenal, AL 35898-5248

RE: Contract DAAH01-98-C-R015
SUBJ: Final Report

Gentlemen:

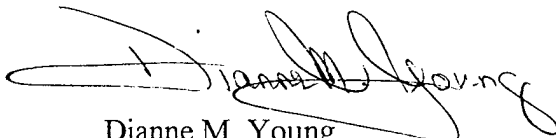
As required by the above referenced contract I am submitting two (2) copies of our final report. I am also enclosing four (4) copies the applicable DD250 for your signature. Please approve this DD250 and send me a signed copy for acceptance.

Please feel free to contact Mr. Michael Hercher for questions of a technical nature, or myself for administrative matters at (978) 887-6600 x111.

On behalf of OPTRA, I would like to thank DARPA for allowing us to participate in the SBIR program.

Sincerely,

OPTRA, Inc.



Dianne M. Young
Contracts Administrator

Enclosures

cc: DARPA, Dr. Pease (1 copy)
DARPA, Attn: AMSAM-RD-CS-R (1 copy report, 1 copy DD250)
DARPA, Attn: AMSAM-RD-WS (1 copy)
DARPA, Attn: OASB/DARPA Library (1 copy)
DARPA, Attn: OASB/SBIR (1 copy)
DTIC, Attn: Acquisitions/OCP (2 copies)
DCMC/GFOM (1 copy DD250)

19980624 030

FINAL REPORT

HIGH SPEED, HIGH ACCURACY STAGE FOR ADVANCED LITHOGRAPHY

Period of Performance: October 20, 1997 - June 15, 1998

June, 1998

Sponsored by:

Defense Advanced Research Projects Agency
U.S. Army Missile Command
AMSMI-AC-CRAY
Redstone Arsenal, AL 35898-5280

Issued by U.S. Army Aviation and Missile Command Under

Contract No: DAAH01-98-C-R015

Submitted by:

OPTRA, Inc.
461 Boston Street
Topsfield, MA 01983
(978) 887-6600

Principal Investigator: Michael Hercher
Engineer: David Mansur

The views and conclusions contained in this document are those of the authors and should not be interpreted as representing the official policies, either expressed or implied, of the Defense Advanced Research Projects Agency of the U.S. Government

OPTRA

REPORT DOCUMENTATION PAGE

Form Approved
OMB No. 0704-0188

Public reporting burden for this collection of information is estimated to average 1 hour per response, including the time for reviewing instructions, searching existing data sources, gathering and maintaining the data needed, and completing and reviewing the collection of information. Send comments regarding this burden estimate or any other aspect of this collection of information, including suggestions for reducing this burden to Washington Headquarters Services, Directorate for Information Operations and Reports, 1215 Jefferson Davis Highway, Suite 1204, Arlington, VA 22202-4302, and to the Office of Management and Budget, Paperwork Reduction Project, Washington, DC 20503

1. AGENCY USE ONLY (Leave blank)	2. REPORT DATE 6/17/1998	3. REPORT TYPE AND DATES COVERED Final Report - Oct 20, 1997 - June 15, 1998
4. TITLE AND SUBTITLE HIGH SPEED, HIGH ACCURACY STAGE FOR ADVANCED LITHOGRAPHY		5. FUNDING NUMBERS DAAH01-98-C-R015
6. AUTHOR(S) Michael Hercher		
7. PERFORMING ORGANIZATION NAME(S) AND ADDRESS(S) OPTRA, Inc. 461 Boston Street Topsfield, MA 01983		8. PERFORMING ORGANIZATION REPORT NUMBER 294
9. SPONSORING/MONITORING AGENCY NAME(S) AND ADDRESSES(S) U.S. Army Missile Command AMSMI-AC-CRAY Redstone Arsenal, AL 35898-5280		10. SPONSORING/MONITORING AGENCY REPORT NUMBER
11. SUPPLEMENTAL NOTES		
12a. DISTRIBUTION / AVAILABILITY STATEMENT Approved for public release; distribution unlimited		12b. DISTRIBUTION CODE
13. ABSTRACT (<i>Maximum 200 words</i>) The overall program goal is to develop an integrated stage and metrology system for microlithography, based on the use of an XY encoder grid, meeting the following specifications: (a) 12" x 12" coverage, (b) accuracy of $\pm 2.5\text{nm}$ or better, (c) operable at a speed of 1 meter/sec, and (d) active control of all 6 degrees of freedom. To this end, the Phase I program had goals of (1) finding one or more suppliers of high-accuracy grids; (2) grid-based measurement repeatability of $\pm 2.5\text{nm}$ or better, (3) ability to work at speeds of up to 1 meter/sec, and (4) development of a short-range optical sensor for servo control of the nominally fixed degrees of freedom (Z , θ_x , and θ_y). With the exception of the velocity specification, these Phase I goals were all met. We were able to work at velocities of up to 790mm/sec, and can readily get to 1 meter/sec by upgrading the speed of the A/D's in our phase processor. Measurement repeatability of $\pm 2.5\text{nm}$ was achieved in an environment where the turbulence-limited repeatability of a laser interferometer was on the order of 10nm to 20nm. We found the Etec ALTA laser-writer to be the best machine for making accurate grids.		
14. SUBJECT TERMS Nanometer, microlithography, metrology, encoder, XY Stage		15. NUMBER OF PAGES 32 16. PRICE CODE
17. SECURITY CLASSIFICATION OF REPORT Unclassified		20. LIMITATION OF ABSTRACT UL

Table of Contents

Section	Title	Page
	Executive Summary	1
A.	Review of overall program goals	2
B.	Targets & Tasks for Phases I and II	2
C.	Phase I accomplishments	3
C.1	Acquisition of an XY grid with uncorrected accuracy of $\pm 200\text{nm}$	3
C.2	Contact printing an XY grid	12
C.3	Calibration techniques for XY grid evaluation	15
C.4	Extend present air-bearing capability to handle 8^2 and 12^2 grids	18
C.5	Prototype short range sensor	19
C.6	Demonstrate 2.5nm repeatability	21
C.7	Demonstrate 1 m/sec velocity capability	24
C.8	Resolution / noise measurement	26
C.9	Evaluation of XY grid made on an Etec ALTA machine	27
D.	Report on NanoGrid marketing and sales	31

List of Figures

Figure	Title	Page
1	Square array	3
2	Diamond Array	3
3	Theoretical diffraction patterns...	4
4	Diffraction patterns from square and diamond arrays	5
5	Turbulence effects on measurement stability	6
6	Linearity error scans on 6" CORE master grid	7
7	Calibration scan for step-and-repeat grid	9
8	Same as figure 7 with step size and reticle reduced by 2x	10
9	Linearity error scans for step-and-repeat XY grid...	11
10	Degradation of contact print quality due to errors...	13
11	Linearity error plots for contact prints of CORE XY master	14
12	Moire test pattern displays	17
13	Moire photograph and superposed interferometer ...	17
14	XY Air bearing stage modifications	18
15	Optical layout of short-range sensor	19
16	Breadboard short-range sensor	20
17a	Short-range sensor theoretical response	20
17b	Short-range sensor measured response	21
18	NanoGrid XY sensor head	22
19	Nanogrid repeatability data	23
20	Onset of velocity errors at 785mm/sec	25
21	Resolution / noise measurement	26
24	Grid made on an Etec ALTA Laser Writer	28
25	Grid made on a Micronic LS200 Laser Writer	29
26	Comparison of grids made on ALTA, CORE, and Micronic...	30
27	NanoGrid lithography	32
28	Interferometer stage	

Phase I SBIR: Final Report

High-Speed, High-Accuracy Stage for Advanced Lithography

Executive Summary

For several years, OPTRA has been developing and advocating the use of an accurate and mechanically stable XY grid, with appropriate readout head, as the optimum metrology solution for microlithography. As wafers and stages get larger, this approach appears to be more and more attractive. It is immune to the turbulence problems of laser interferometers, is more compact, less vulnerable to Abbe errors, and less expensive.

In this Phase I Final Report we show:

- Resolution at the nanometer level;
- Repeatability at the 2 to 3 nanometer level; and
- The ability to work reliably at speeds of up to 750mm/sec, with the prospect of going to 1 m/sec without undue difficulty.

We have also qualified the Etec ALTA machine for the manufacture of 8-inch square XY grids of excellent quality (high accuracy, no high spatial frequency errors), and are close to qualifying a second vendor for the manufacture of a 12-inch XY grid of comparable quality.

To get the full benefit of this approach to stage metrology, the metrology system must be incorporated into the stage design from the very beginning. With the proper design, stages may be much lighter than they have been in the past – which means they can move faster and with less power dissipation.

This program has given us the opportunity to demonstrate these capabilities in a complete system, which is the only way that semiconductor capital equipment manufacturers can be persuaded to explore the possibilities of a radically different and, in our opinion, better metrology system for the positioning large stages with nanometer repeatability.

Phase I Final Report

High-Speed, High-Accuracy Stage for Advanced Lithography

A. Review of Overall Program Goals

The goal of this program is to develop a combined XY stage and metrology technology designed to meet the anticipated requirements for semiconductor lithography on 12-inch wafers. Critical requirements include:

- 12" × 12" coverage;
- ±2.5nm accuracy;
- velocity up to 1 meter/sec; 100msec turnaround; and
- active control of all degrees of freedom.

To meet these requirements we have proposed an XY-grid-based metrology system with sub-nanometer resolution, an air-bearing stage, and the development of a short-range optical sensor with a 20nm dynamic range and sub-nanometer resolution for monitoring nominally fixed coordinates (pitch, tilt, and height).

B. Targets & Tasks for Phases I and II

The table below shows the key tasks planned for Phases I and II:

Phase I	Phase II
1. Get an 8" square grid with uncorrected accuracy of ±200nm or better.	1. Design a lightweight integrated stage & metrology system for 12" travel.
2. Develop a grid calibration protocol and use it to calibrate the 8" grid.	2. Develop a low-cost technique for accurately replicating 8" to 12" grids.
3. Expand our air-bearing stage to handle 8" and 12" square grids.	3. Carry out market research to define required stage/metrology features.
4. Design & build a prototype short-range sensor with ±2.5nm repeatability.	4. Build prototype XY stage with active control of all 6 coordinates.
5. Demonstrate 1 m/s stage velocity & 0.1 sec turnaround (stage & metrology).	5. Work with a beta-site client to perfect overall system performance.
6. Demonstrate repeatability of ±2.5nm.	6. Show compliance with target specifications.
7. Evaluate fidelity of contact prints from high-accuracy grid masters.	

In defining these tasks, we have first identified what we regard as the critical problems to make sure that they are addressed in Phase I. Thus the issues of grid fabrication and calibration, grid replication, and high speed data processing are all in Phase I.

Progress to date on each of the Phase I tasks is described in the following sections.

C. Phase I Accomplishments

C.1 Acquisition of an XY Grid with an uncorrected accuracy of $\pm 200\text{nm}$

This is somewhat of a chicken and egg problem: we need an excellent metrology system to fabricate a highly accurate grid... so that we can assemble an excellent metrology system. Of course, even an inaccurate grid will have the virtue of high repeatability, and can thus in principle be calibrated to achieve the desired degree of accuracy. In practice, however, a grid which is accurate without correction is highly desirable; in particular we want a grid whose corrections do not have high spatial frequency components. This is so that the correction table will not be excessively large, and so that there is no requirement for a very precise fiducial mark (to initialize the correction process).

Our XY grid has a spatial period of 10 microns in both X and Y. The design we have chosen to use is shown below in figure 1. It consists of an array of 5-micron chrome-on-glass squares separated by 10 microns in both X and Y. An alternate design is shown in figure 2. Desirable features of the grid design include:

- High efficiency: lots of light in the ± 1 diffracted orders
- Low zero-order intensity
- Ease of manufacture
- Ease of replication or contact printing (the second design below excels in this regards, since the positive and negative images are interchangeable)

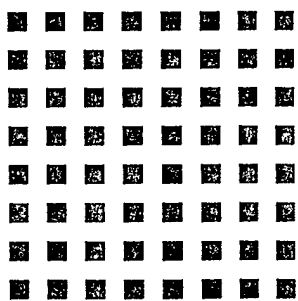


Figure 1 Square Array

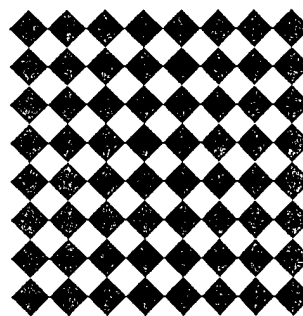


Figure 2 Diamond Array

Our choice of design was based on the combination of relatively high ± 1 order efficiency, and low zero-order content. An ideal grid would be a phase grating based on the second design, with a phase difference of π between the array of squares and the background (this would eliminate the zero order entirely, putting most of the light in the ± 1 orders).

Figure 3 shows theoretical plots for the diffraction patterns for the designs in figures 1 and 2, and figure 4 shows photographs of diffracted light patterns from the same two array designs.

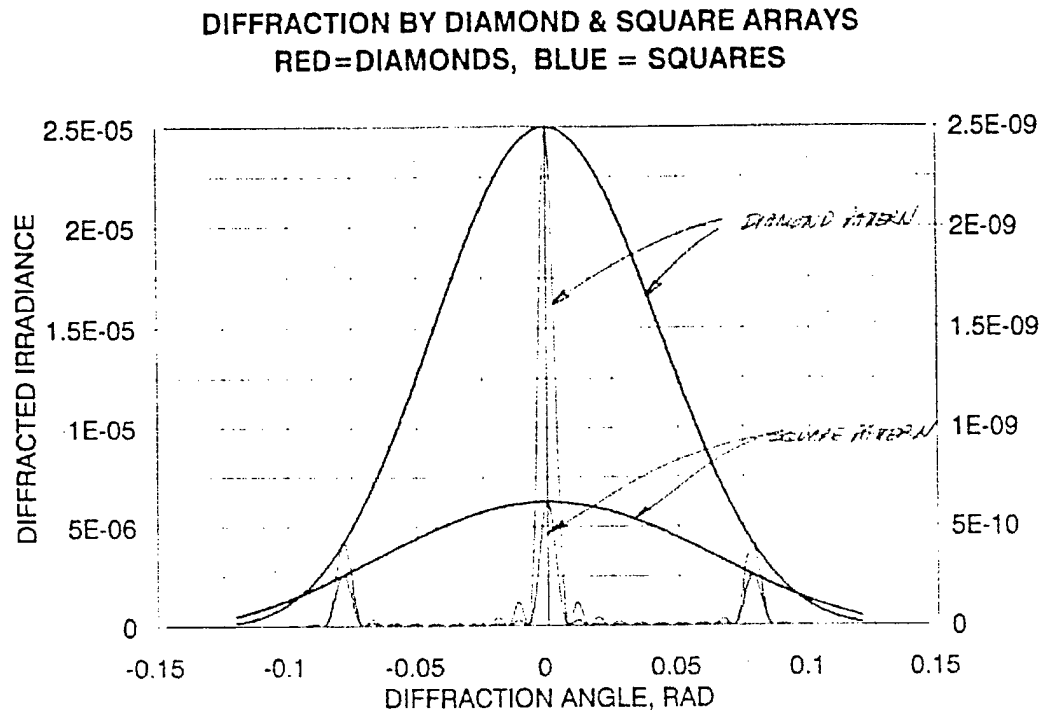


Figure 3 Theoretical diffraction patterns for square and diamond arrays

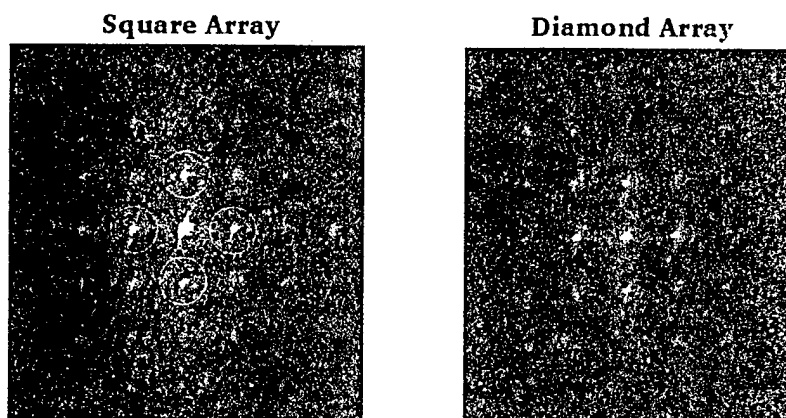


Figure 4 Diffraction patterns from square and diamond arrays (see figures 1 and 2). Only the ± 1 diffracted orders are used (these are circled in white on the left).

With regard to fabrication of the grid, the requirements are somewhat different from those for typical semiconductor microlithography. When IC's are being fabricated, there is generally little concern for long range accuracy, and a lot of concern for the fidelity of line-widths and other fine detail. In our case, we are very concerned with long-range accuracy, and not so concerned with the exact size or shape of the squares in the pattern. We could even tolerate some missing squares. (We look at about 200 squares at any given instant.) What we really care about is the constancy of the spacing between the squares.

In our first experience with making linear scales of this type, we found that the commonly used step-and-repeat process, in which a photo-reduced master scale segment was contact printed onto the encoder and then moved under laser interferometer control to its next position, was not very accurate. Scale manufacturers generally calibrated their encoders at intervals of 0.5" to 1" and in most instances when they saw our data it was the first time they had really seen what their encoder accuracy was like.

There were two immediate problems. First, the magnification used in photo-reducing the master scale segments was not precisely controlled (an error of 1 part in 10^5 is significant), resulting in butting-errors where adjacent contact prints met. Second, although the laser interferometer could control the steps to within 50 or 100 nanometers, there were still random errors in where the master-scale was placed after each such step. The use of a projection system to replace contact printing addresses the latter problem, but not the former.

There are other problems as well. One of the primary forces driving our work with a grid-based metrology system is the problem of turbulence that is commonly encountered in laser interferometry in all but the most highly controlled environments (e.g. a vacuum). In a quiet laboratory setting, turbulence typically creates an interferometric

measurement uncertainty of about $5\text{nm}/\sqrt{(\text{cm of uncompensated optical path})^1}$. Thus if one arm of the interferometer has a 60cm uncompensated path, as would be the case for a 300mm stage at one extreme of its travel, there would be an rms uncertainty of about 40 nm in the measured position of the stage. Figure 5 illustrates turbulence fluctuations in an interferometric measurement, and also shows the relative measurement stability of a grid based position measurement.

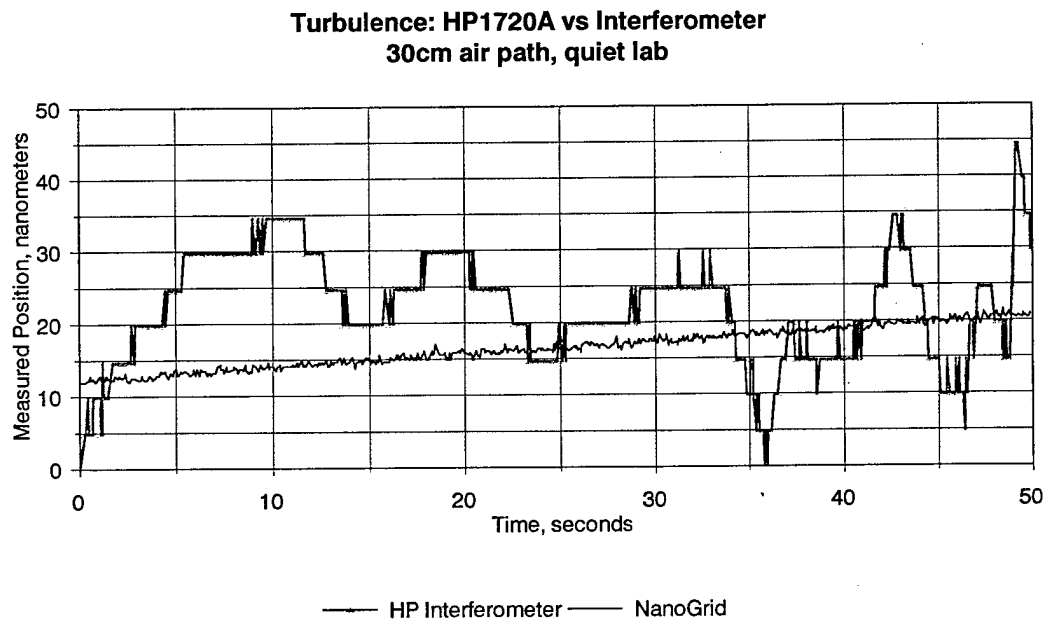


Figure 5 Turbulence effects on measurement stability

The Etec Corporation manufactures a number of e-beam and direct laser-write micro-lithography machines for making masks and reticles. These machines, in our judgment, define the state of the art. Their CORE machine claims an accuracy of 80nm over a 6-inch square field. This machine uses high-speed mirrors to scan multiple laser beams over the writing area, and turns the beams on and off with acousto-optic modulators. The entire machine is in a highly controlled environment, and differential interferometers are used to directly monitor the relative position of the projection optics and the stage which carries the photoresist-coated substrate (this is in contrast to most laser interferometer stages, where the interferometer is attached to the base and a "rigid" structure fixes the relative positions of the base and the projection lens).

We have had both linear encoders and 6-inch XY grids made by CORE machines, and we have measured accuracies of about 100nm — including the effects of turbulence in the laser interferometer used to make independent measurements of the encoder or grid

¹ We don't have a reference for this value, but it is consistent with many observations that we have made over a wide variety of optical paths. If the laboratory is not quiet (e.g. if the interferometer mirror is moving, or if people are talking in the laboratory, the turbulence errors are larger).

position.² Figure 6 shows arrays of calibration plots for a CORE-made XY grid. We believe — and have demonstrated (see section C.6) — that the much of the noise on these plots is due to turbulence in the laser interferometer.

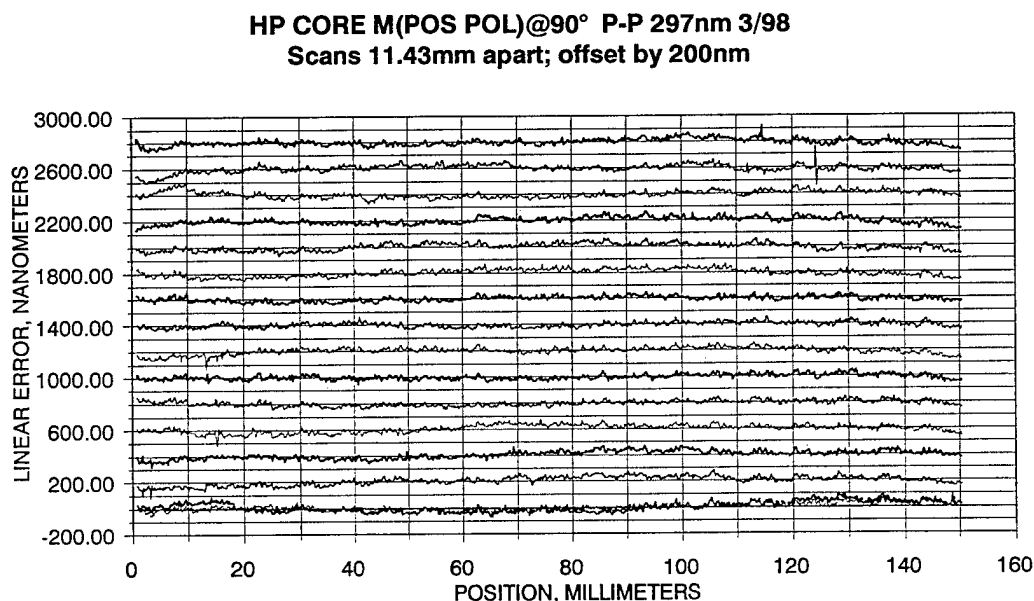
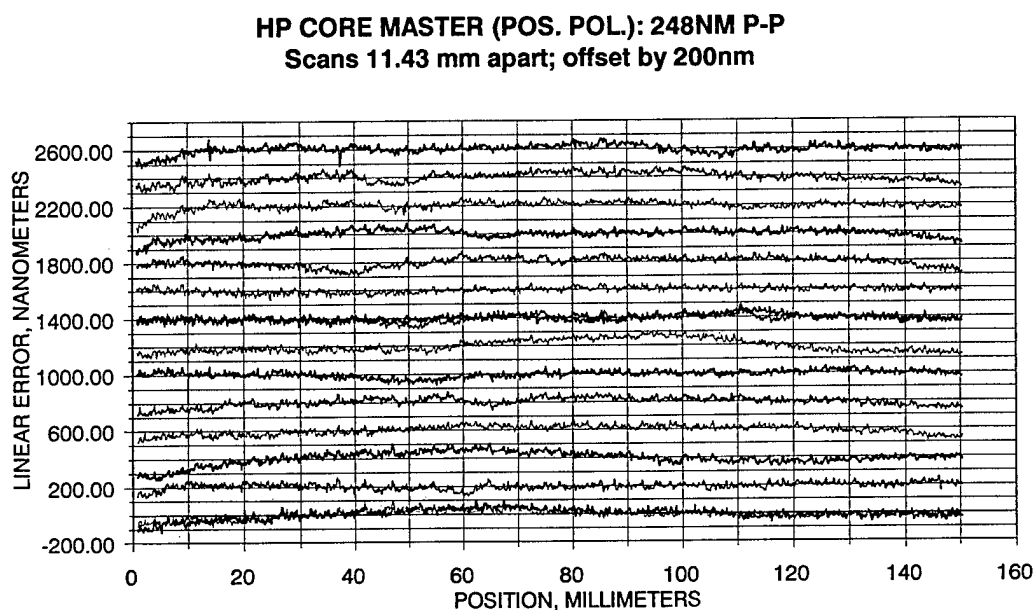


Figure 6 Linearity error scans on a single 6-inch square XY grid made on an Etec CORE machine (direct laser write). The grid is of excellent quality; we believe that most of the noise apparent in these scans is due to air turbulence effects on the laser interferometer used for calibration.

² The procedure used to obtain calibration data for these XY grids is described in Section C.3.

Direct-write grids written on the Etec CORE machine were of excellent quality and comfortably met both our 200nm accuracy requirement, and our desire for minimal high-spatial-frequency content in the calibration curves. However, the CORE machine can only be used to write patterns that fit inside a 7-inch square. Etec has recently made the ALTA 3000 and 3500 machines, which are also direct-laser-write machines but which can write areas of up to 8.5" square, and for which they claim an accuracy of $\pm 30\text{nm}$. These machines require quartz (fused silica) substrates that are flat to 2 microns over their entire area.

Our plan for getting an 8" grid (actually 215mm \times 215mm) was always to have it made on an ALTA machine. These machines, however, are very expensive, few in number, and are being used full-time to make masks and reticles for high-density IC's. We have found ALTA machines at the following locations: DuPont (Texas), Photronics (California and Texas), Siemens (Germany), and IBM (New York), but had been unsuccessful until very recently in getting onto one of these machines to make one or two 8-inch XY grid masters. We were forced, therefore, to explore the use of XY grids made using more conventional step-and-repeat lithography.

The Step-and-Repeat Process

In a typical step-and-repeat process for making an accurate grid, a 1.5-inch square grid reticle is made at 5 \times (i.e. with 25-micron squares on 50-micron centers), and is then projected onto the final grid substrate at 0.2 \times . The substrate is stepped in 0.3-inch increments and repeated exposures are made. The 5 \times reticle is made by projecting a single square and stepping the reticle under laser interferometer control. On a 215mm square grid there are more than 460 million 5-micron squares; within the 0.3-inch square area cover by a single stepped exposure, there are just over 0.58 million individual squares. Over 800 stepped exposures are required to cover the complete grid area.

The stepping pattern typically starts at one corner and steps the width of the plate in one direction (say the x-direction), in 0.3-inch increments, under laser interferometer control. If stacked stages are used, the x-stepping direction involves the upper stage to minimize the weight that has to be continuously stepped. At the end of the first row of stepped exposures, the stage is returned to its starting position and the stage is stepped by 0.3-inches in the y-direction and the sequential stepping process in the x-direction is repeated.

Figure 7 shows calibration plots made from an early attempt to make an accurate XY grid using a step-and-repeat camera at HTA Photomask in San Jose, CA. The caption to this figure discusses the salient points in some detail. In summary, these data show:

1. There is an average butting error of $\approx 460\text{nm}/\text{step}$ (7.6mm step); this could be accounted for by a projection magnification error of 6 parts in 10^5 ;
2. The standard deviation for the butting error is $\approx 410\text{nm}$;

3. Within each stepped pattern there is a small but very repeatable variation in magnification (as evidenced by the repeatable curvature of the segments of the calibration plot; this is probably due to distortion in the projection lens).
4. The peak-to-peak non-linear error for this calibration scan was approximately 2000nm.

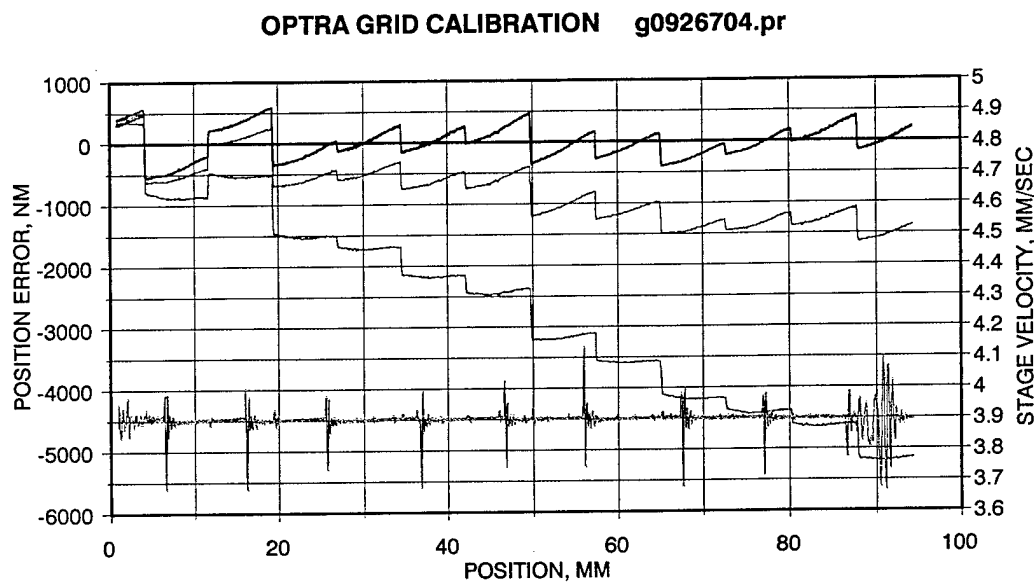


Figure 7 Calibration scan for an XY grid made using the step-and-repeat lithography process.

All three plots show the same data, but with different slope constants (the horizontal plot along the bottom shows the stage velocity, so that we could make sure that features in the error plots were not due to velocity perturbations).

In the lower stair-case-like plot, the slope constant has been adjusted to linearize the data within each step. The significant features are (a) the well-defined slope of the stair-case, corresponding to a well-defined mean stepping error of about 460nm, and (b) the significant deviations from this mean stepping error — the third step even went in the wrong direction. The curvature of each step is probably evidence of a small amount of distortion in the projection lens. The projected size of each reticle exposure was 0.3"×0.3" (7.62mm×7.62mm).

Following assessment of these and similar data, we masked the projected reticle by a factor of two (i.e. we reduced its projected size from 7.6mm × 7.6mm to 3.8mm × 3.8mm) and attempted to improve the vibration isolation of the camera. This was intended to reduce the average butting error by a factor of two to reduce the effects of distortion within each stepped exposure, and to reduce the standard deviation of the butting errors. The results of these changes are shown in figure 8. The results were:

1. The mean stepping error was reduced to 220nm;
2. The standard deviation of the stepping errors was reduced to 150nm;

3. The effects of distortion in the projection lens were greatly reduced; and
4. The peak-to-peak accuracy error was reduced to $\approx 800\text{nm}$.

On the other hand, there were twice as many discontinuous jumps in the calibration curve because there were twice as many steps. We should note, however, that these jumps are not really discontinuous. Because the XY Grid sensor head has an optical footprint of about 120 microns (i.e. it averages over an area of about 0.014mm^2), abrupt transitions on the grid are smoothed out when the grid position is read out by the sensor head. Expressed in different terms, the readout sensor effectively serves as a low-spatial-frequency pass filter with a cut-off at about 8 lines/mm.

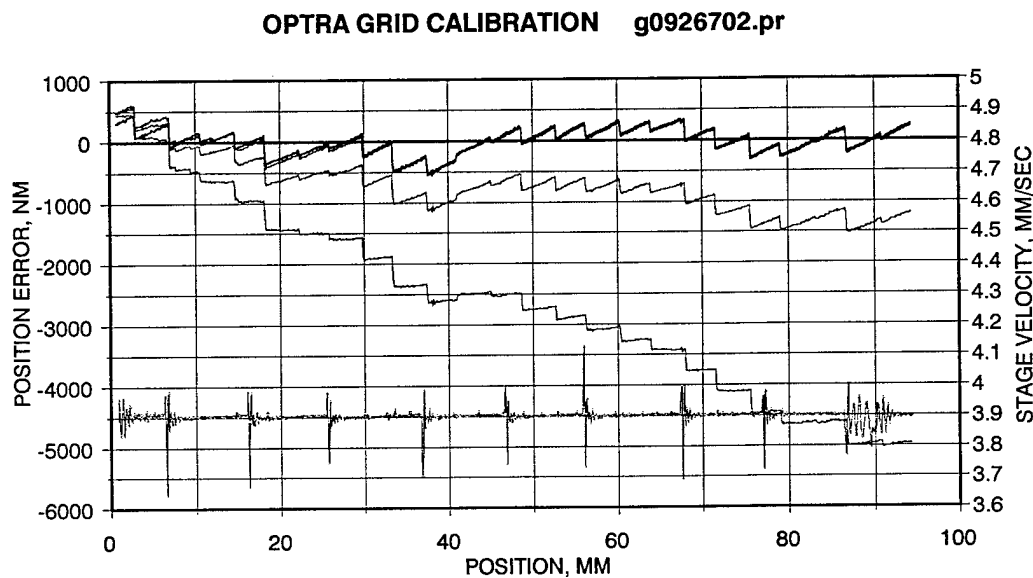


Figure 8 Same as figure 7, but with step size and reticle size reduced by 2x.

A second mask-making vendor (Photonics, Colorado Springs, CO) was approached and made a series of 8" step-and-repeat grids for us. The results were very similar to those obtained by HTA, even though their equipment was entirely different in its structure and operating protocol. By working closely with Photonics, we were able to correct the interferometrically-controlled step size to compensate for projection magnification errors, but as shown in figure 9, the residual random component of the butting error resulted in a peak-to-peak accuracy for across-the-grid scans to a value of between 600nm and 800nm.

We have invested a lot of time in exploring the prospects for improving the quality of a step-and-repeat grid. The bottom line is that to achieve our accuracy and calibration goals, we should make our master grid on an ALTA machine and, if ALTA grids are too

expensive for production, we should figure out how to replicate them with acceptable fidelity.

Largely as a result of the rapport we developed with the LAM (Large-Area-Mask) group at Photronics, we were finally able to schedule the fabrication of an 8.3-inch square grid on an ALTA machine at Photronics in Sunnyvale, CA. OPTRA will supply the quartz substrate, flat to 2 microns, Telic Inc. will deposit the chrome and then spin on the photoresist, Photronics Sunnyvale will write the grid using their ALTA machine (which they have had to upgrade to handle the full 8+ inches that we require), and Photronics Colorado Springs will process the plate.

STEP AND REPEAT: GRID CALIBRATION
Scans 11.43mm apart; offset by 200nm

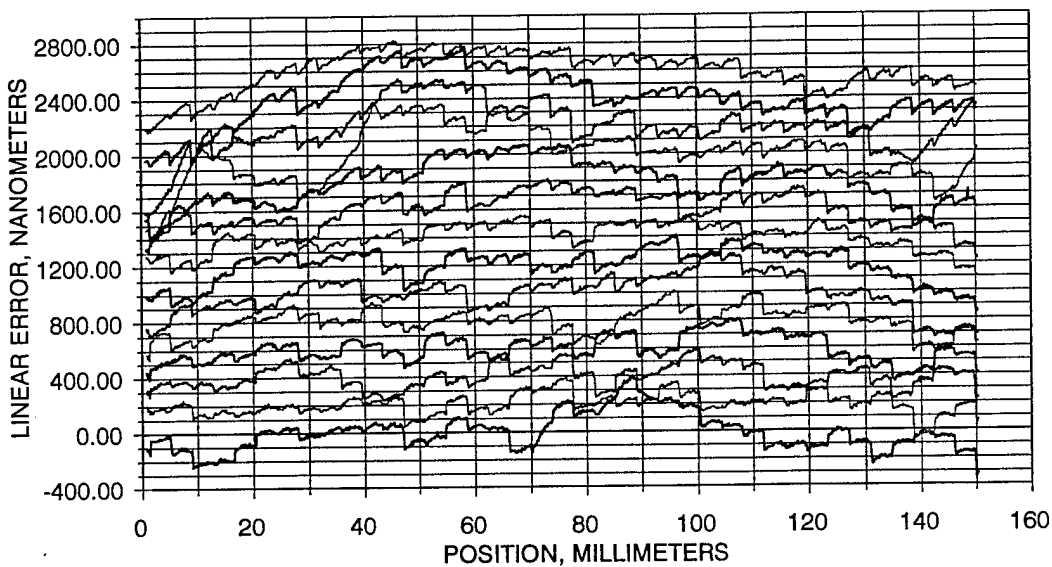


Figure 9 Linearity error scans for a step-and-repeat XY-grid after correction of the step size to minimize butting errors. The mean butting error has been reduced to close to zero, but the residual random stepping errors result in peak-to-peak linearity errors on the order of 600nm.

The problem getting a grid written on an ALTA machine is that the ALTA machines are in great demand and are very profitable for their operators. The owners of these machines are understandably reluctant to break into their product-run schedule to handle a non-standard job — without the prospect for much repeat business — for a small company that is setting tight specifications. Fortunately, the grids we have had made and have analyzed to date have given the Photronics LAM group useful information about their own metrology and its limitations, and in return they have been extremely helpful in getting us onto their ALTA machine in Sunnyvale.

We expect to have an 8.3" master grid in hand and tested by the beginning of May, 1998. If past experience with grids made on the Etec CORE machine is any guide, the new master grid will be better than our ability to calibrate against a laser interferometer. We describe how we plan to improve our testing in a later section. (*Note: this section was written in March 1998; for an account of the saga of the ALTA grid, see section C.9).*

C.2 Contact Printing an XY Grid

One of the great advantages of a relatively coarse metrology grid (in contrast to a holographic grid, which may have a spatial frequency of more than 1000 lines/mm) is that it is theoretically possible to make a contact print from it and thereby obtain inexpensive replicas of an expensive master grid. Note, however, that expensive as our master grid will be, it doesn't come close to the cost of an accurate interferometer L-mirror for use on an 8" stage.

Early in Phase I we had a contact print made of a 6" grid which had been made on a CORE machine. Our goal was to compare the accuracy of the contact print to that of the master. The results of this test are shown in figure 10. Although there has clearly been some spatially random degradation in accuracy (about 100nm to 300nm in magnitude), and a smooth curve in the non-linear error plot in one portion of the plate, we choose to find these initial results quite promising. We believe that the smoothly curved error component is probably due to either a chrome bump on the master plate, or a piece of dirt between the two plates — probably just outside the exposed grid area.

The major requirements for good fidelity in a grid contact print are (1) very close proximity of the master grid and the contact substrate, (2) good collimation of the light source (i.e. the illuminating light should be normal to the master grid over the entire field of view), and (3) small angular subtense of the light source. *Non-uniformity of the illuminating direction converts separation between the master and contact substrate into grid position errors.* This point is illustrated in figure 11. The collimation requirement is more critical to us than the angular size of the source, since a finite source size blurs the edges of features rather than moving their centers. Similarly, exposure errors may change the size of the individual squares, but will not change their locations.

In some respects our contact printing requirements are quite different from those of more conventional users. In particular, we are very concerned with long-range accuracy, and not very concerned about fine detail and high definition. We will be obtaining contact prints of the master grid starting in May, 1998, and evaluating them in terms of both accuracy and cost. It is quite possible that we will decide that it would be a sound investment for OPTRA to get into the business of making our own contact prints, using equipment designed and/or modified to meet our particular requirements. Certainly, any modifications to the contact printing process that would allow us to relax the tolerance on substrate flatness would pay very large dividends in terms of lowering the ultimate cost of a grid-based metrology system.

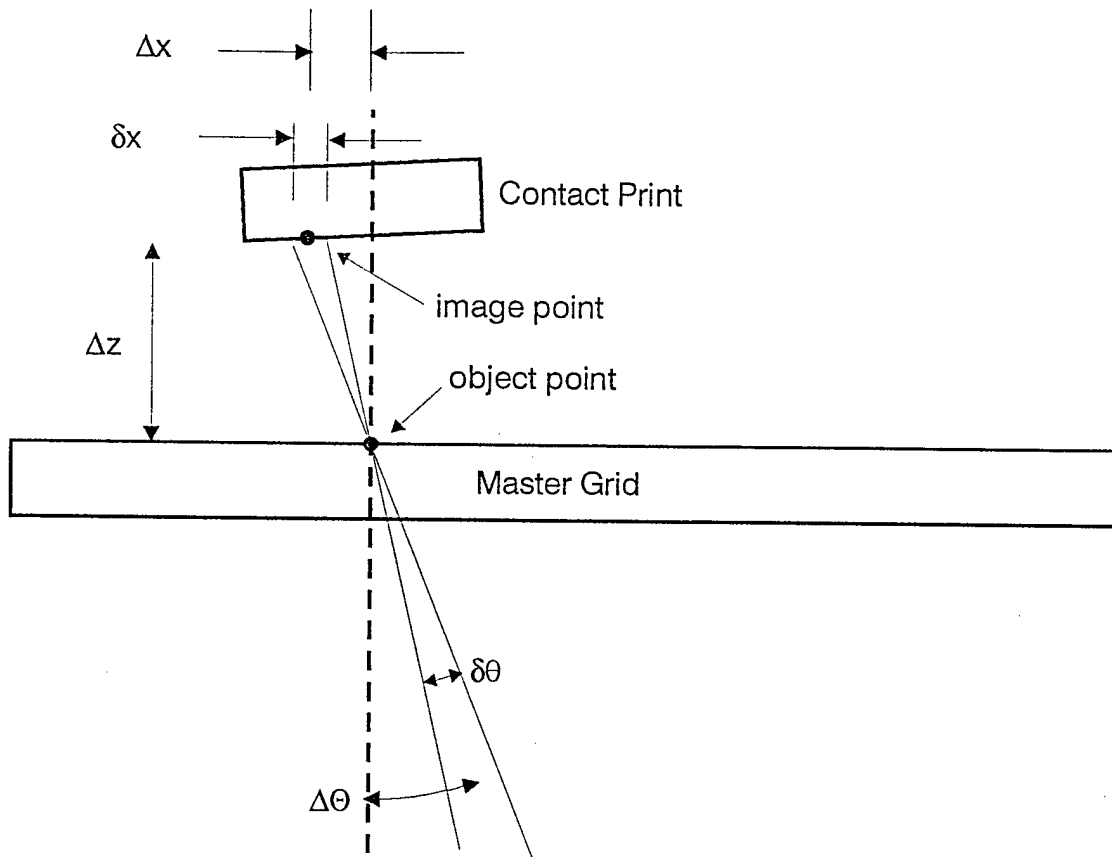


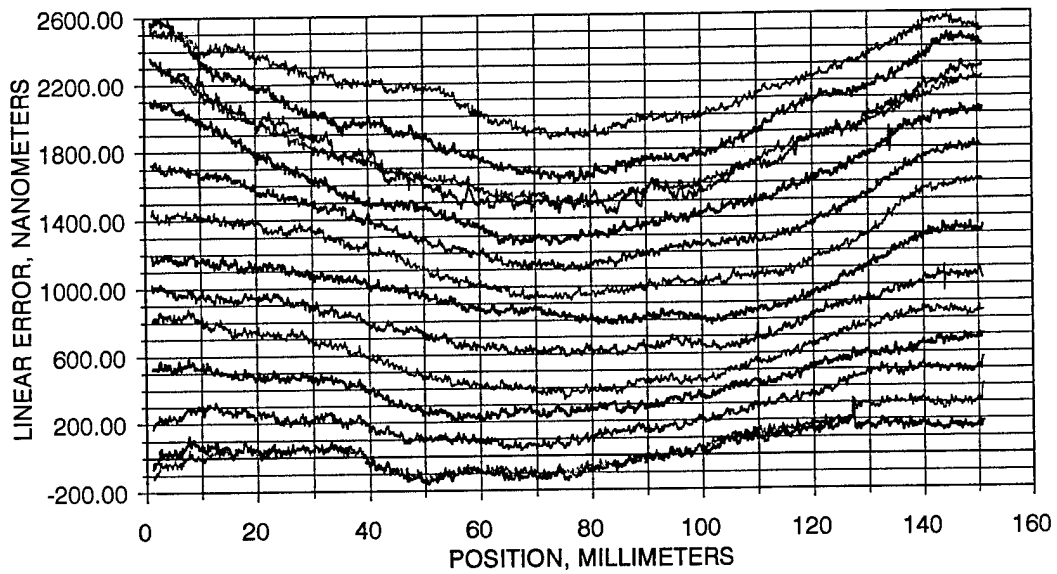
Figure 10 Degradation of contact print quality due to errors in plate proximity, finite source size, and collimation errors.

Ideally, the two plates would be in perfect contact, and the image would have perfect fidelity. The combined effects of a finite spacing between the plates (Δz), a finite angular source size $\delta\theta$, and a collimation error, $\Delta\theta$, produce images position errors (Δx) and a spread in the image of a point or narrow line (δx). The two errors are given by:

$$\Delta x = \Delta z \Delta\theta, \text{ and } \delta x = \Delta z \delta\theta,$$

respectively. For high-fidelity grid replication, source collimation is critical. Flat, clean plates can however give good copies even without perfect collimation.

HTA CONTACT/HP MAS. @180: 1/27/98
11mm apart; offset by 200nm,1&10repeat



HTA1 CP@90°; fr CORE M; P-P 427nm 1/98
11.43mm apart; os 200nm;repeat 1,7&11

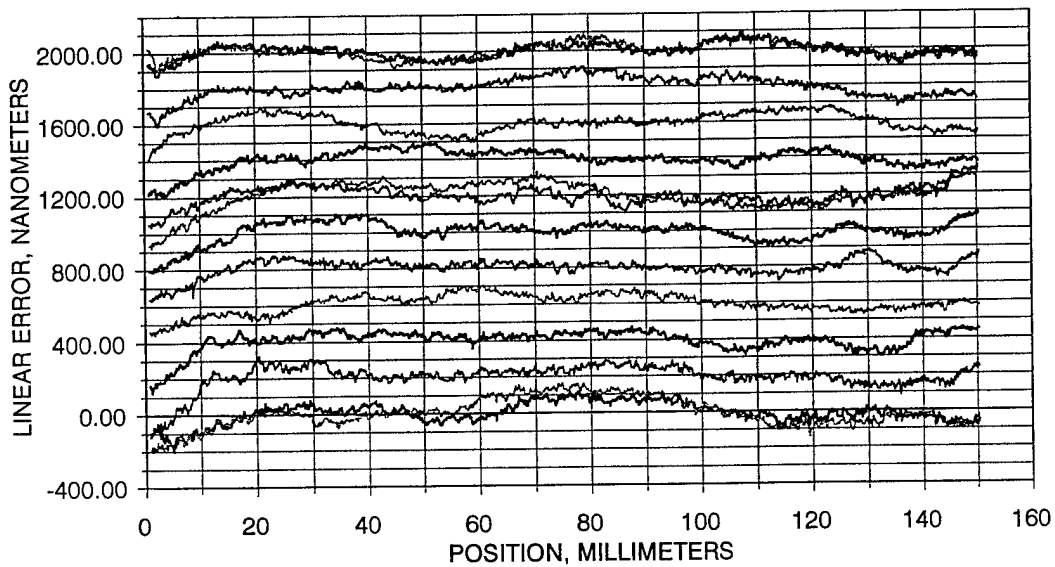


Figure 11 Linearity error plots for a contact print of a CORE XY-grad master
(compare to CORE master plots in figure 6).

C.3 Calibration techniques for XY grid evaluation

The stage calibration algorithm described by Ye, Takac, Berglund, Owen, and Pease is an elegant and in many ways ideal technique for calibrating an XY stage at an array of points, and to then extend the calibration to all points by using orthogonal Fourier series.³ This approach is particularly suitable for stage errors that are uniformly distributed and quasi-random. However, grids made using the step-and-repeat process don't meet these criteria. Their errors have high spatial frequency content, and might be missed entirely by a calibration process based on a fixed array of points. We have developed two different approaches to error assessment and calibration for grids of this type: (1) an array of continuous linear scans in which grid-based data is compared to interferometer-based data, and (2) moiré testing in which the grid under test is compared to a grid of known quality.

Linear Scans

Our most accurate technique for characterizing the accuracy of an XY grid is to make a series of linear scans across the plate (say in the x-direction) at different y-positions. We have an air-bearing stage with a plane interferometer mirror (which can monitor displacements in the x-direction at different y-positions), and can accurately mount the grid encoder on the stage so that the x-grid-axis is well aligned with the stage x-axis. The stage is clamped so that it cannot move in the y-direction. The stage is then driven in the x-direction at about 4mm/sec and position data are synchronously clocked out from both the laser interferometer and the grid x-position sensor at 780Hz. These data sets are averaged and reduced from 30,000 points to 1000 points, covering a measurement range of 150mm (so that the interval between the final data points is ≈ 150 microns — approximately the size of the measurement footprint). Next, a linear regression is done on the data, with the laser-interferometer position being the independent variable and the grid position being the dependent variable. This spreadsheet regression gives us a *constant* and a *slope*, plus a measure of the quality of the fit of the data to a straight line. The straight line passing through the interferometer position axis at the constant value and having a slope equal to the slope value is the best linear fit of the grid data to the interferometer data. Finally, we plot the difference between the grid data and the best-fit straight line to get the *linearity error* data, or simply the error data. We are not particularly concerned with the value of the slope (ideally equal to unity), but are concerned with the departures from linearity. All of the linear error data presented in this report were obtained using this protocol.

By making a series of scans in the x-direction at an array of y-values, we can map out the linearity errors fairly thoroughly. If a step-and-repeat lithography process has been used, the y-intervals should equal the step-size (so that every projected copy of the reticle is sampled), and the scans should go down the centers of the stepped projection prints. The

³ J.Ye, M.Takac, C.N.Berglund, G.Owen, and R.F.Pease, "An exact algorithm for the self-calibration of two-dimensional precision metrology stages," *Precision Engineering* **20**, 16-32, 1997.

grid is then rotated 90°, trued up to the direction of motion of the stage, and another set of data taken for the y-direction on the grid (at an array of x-values).

The advantage of this approach is that it can be carried out fairly quickly under computer control, and it gives an accurate picture of the overall grid errors including their high spatial frequency content. From our point of view, this technique has the further advantage that it does not require an expensive L-shaped interferometer mirror (or even a very flat plane mirror), which we don't have. Its disadvantage is that it gives no direct information about the orthogonality of the grid rulings. Fortunately, the grid orthogonality can be easily assessed using the moiré techniques described below.

Moiré pattern grid assessment

Linear encoders are conventionally used with read-out heads based on a moiré pattern. When identical encoders are superposed they have a transmission of between 0 and 50% depending on the relative phase of the two encoders. As one encoder is moved relative to the other, the transmission is modulated — one cycle of intensity modulation for each spatial period of relative motion.

When an XY grid of known high quality is placed adjacent to an unknown grid and carefully aligned to it, the transmission will be spatially uniform if the two grids are identical. Spatial variations in the transmission of the pair of grids indicate that there are spatial variations in the relative phases of the two encoders. The relationship between transmission and relative phase is not linear; it depends on the shape of the encoder profile, the proximity of the two grids, and the degree of collimation of the light source. Nevertheless, the moiré pattern gives a very clear qualitative picture of the distortions in the unknown grid and allows grids to be very quickly evaluated. The beauty of a moiré test is that the entire grid is assessed and recorded in parallel. If the grid is moved by ¼-cycle (in both x and y) between moiré pattern records, then fairly accurate grid assessment is possible. The use of false color or false grayscale (figure 12) makes visual assessment of the moiré patterns easier. Figure 13 shows a moiré pattern superposed on a linear scan to illustrate the relationship between the information obtained by these two techniques.

Quick check for orthogonality: In the moiré pattern there is one cycle of intensity modulation for a 10-micron displacement of one grid relative to the other. For a 4-inch square moiré pattern, the two grids must be aligned in angle to within about $(2.5\mu\text{m}/4" \times 25,400\mu\text{m}/\text{inch}) = 0.000025$ rad (5 arcsec) to make the field visually uniform in intensity. If one of the grids is then rotated by 90° and can then be aligned again to make the field of view uniform in intensity, there is an assurance that each of the two grids is orthogonal to within 5 arcsec or better.

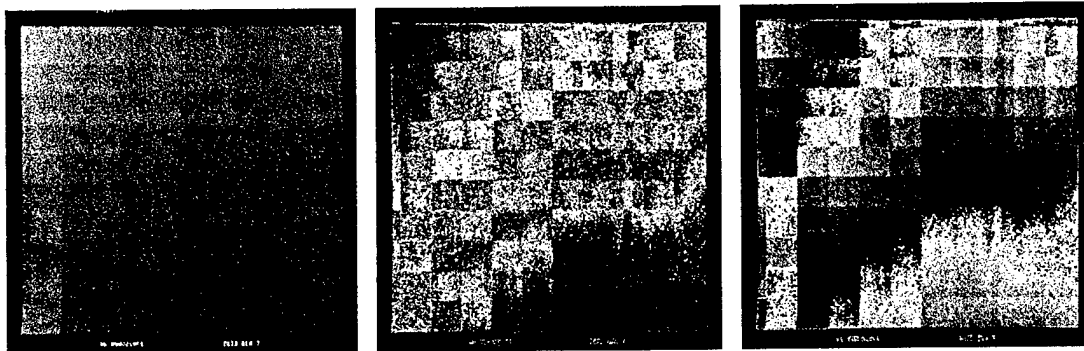


Figure 12 Moire test pattern displays

The left-hand figure shows the originally recorded moire pattern between a step-and-repeat grid and a 4" reference grid made on an Etec CORE machine. The uniform component of the intensity gradation is due either to a constant linear scale difference between the two grids, or an error in their relative angular orientation. The figure in the center is a false-color image of the same photograph (different color assigned to each of the 256 gray levels), and the figure on the right is a false gray-level photograph in which the original 256 gray levels were mapped into four 64-gray-level blocks each running from black to white.

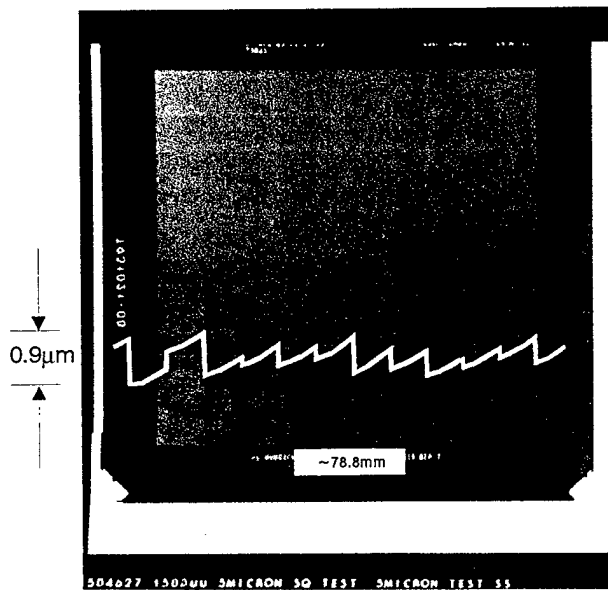


Figure 13 Moire photograph and superposed interferometer calibration curve

The Moire pattern was obtained by placing a 4" square reference grid (obtained using an Etec CORE laser plotter) on top of a single-stepped test grid, and carefully aligning the two to "fluff out" the spatial beat pattern between the two. Both grids consisted of nominally 5 micron chrome squares on 10 micron centers.

The interferometer calibration curve was obtained by putting the test grid on an air-bearing XY stage, equipped with a plane mirror for interometric testing, and simultaneously reading the stage position with a laser interferometer and with a NanoGrid sensor head. The plot shown is the difference between the actual NanoGrid data and a linear regression of the NanoGrid data to the interferometer data.

C.4 Extend present air-bearing stage capability to handle 8" and 12" grids

The present OPTRA air-bearing stage is equipped for servo-controlled motion over a 6" × 6" area. We are designing modifications to the stage so that it can hold substrates up to 13" square, and servo-control their motion over a range of 12" × 6". Thus the modified stage would allow us to calibrate grids of up to 12" (300mm) in size. These modifications were implemented by the end of April, 1998. Figure 14 illustrates the changes in the stage design (lengthen the stage bed, extend the range of one of the linear motors, and add provision for a second XY read-out head). The latter modification (provision for a second read-out head) will allow us to validate resolution and repeatability without the turbulence noise and 5nm LSB of our laser interferometer.

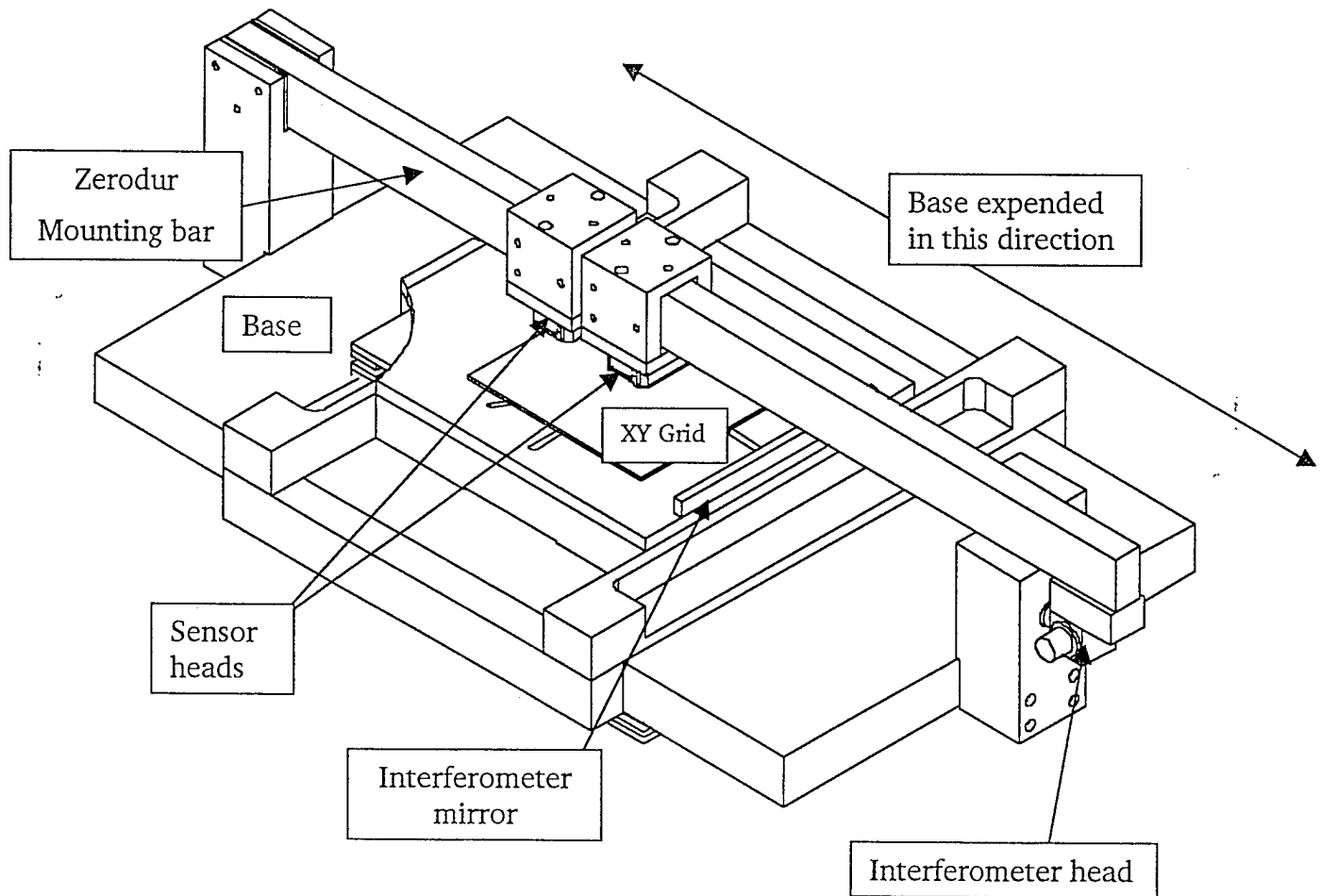


Figure 14 XY Air-Bearing Stage modifications

C.5 Prototype Short Range Sensor

The SRS (Short Range Sensor) is intended to provide high-resolution position information over a relative short range. We have designed an optical SRS which is analogous in function to a capacitance gage, but which has a number of advantages:

1. Relatively insensitive to temperature;
2. Linear response over a significant portion of its range;
3. Immunity to electro-magnetic interference;
4. Can sense the position of a non-conducting surface (e.g. uncoated glass); and
5. Can operate with a physical separation of up to several millimeters.

Figure 15 shows the optical layout of this sensor.

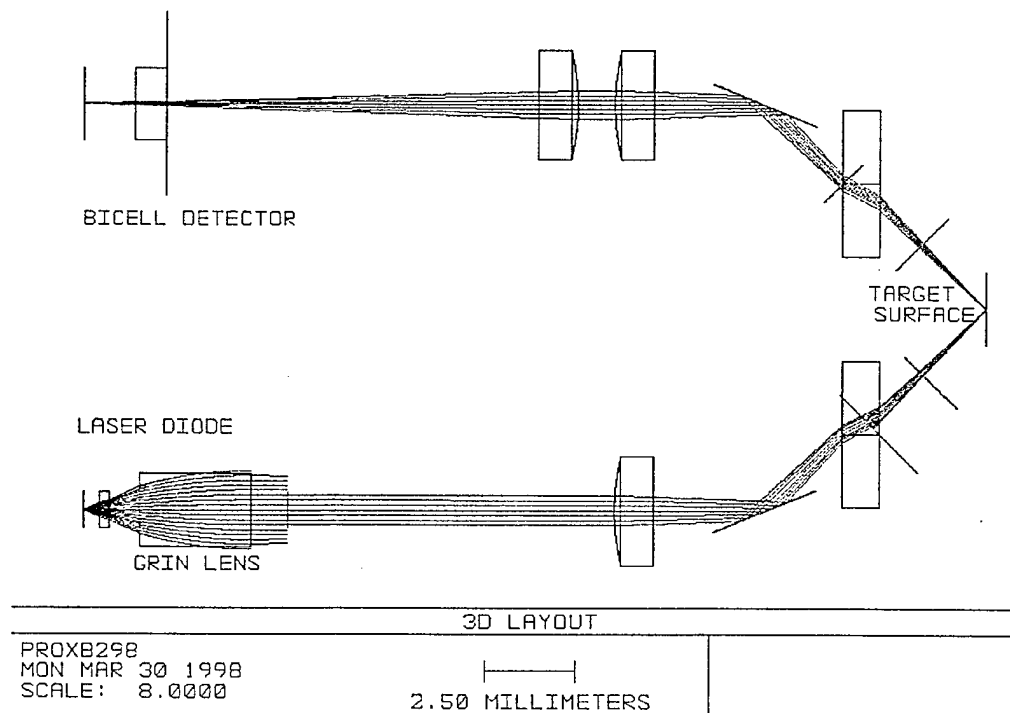


Figure 15 Optical layout of Short Range Sensor

As can be seen from this figure, left or right displacement of the target surface results in a vertical displacement of the imaged laser spot on the bicell detector. If the two signals from the bicell detector are A and B, then the image displacement (and hence the displacement of the target surface) is proportional to $S = (A-B)(A+B)$. The relationship between surface displacement Δz and signal S is linear over a range of approximately $D/2$, where D is the aberrated image size at the detector and where we have assumed a magnification on the order of unity. As we have designed the optics, the spot size of the image on the detector is about 30 microns, so that we have a linear measurement range of approximately 15 microns.

With regard to measurement sensitivity, the system was designed to be close to shot-noise limited and this was confirmed in measurements with the breadboard sensor shown in figure 16.

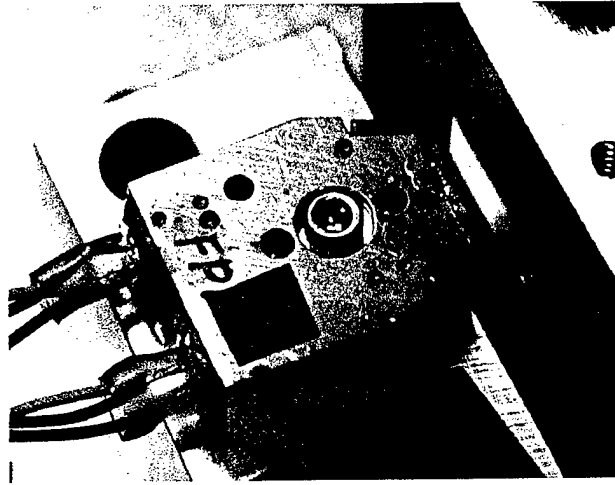


Figure 16 Breadboard Short Range Sensor

This sensor was linear to within 1% over a 10 micron range, has a noise equivalent displacement of under 5nm for a 10kHz measurement bandwidth, and had a capture range of approximately 100 microns (the range within which a servo can be locked). The theoretical response of SRS sensor is shown in figure 17A, with spot size as a parameter, and experimental calibration data is shown in figure 17B.

Although the short-range sensor is a useful and sensitive position sensor, it excels as a null sensor – serving to keep a servo-controlled dimension at a preset value. We intend to use this sensor to monitor the Z-position of the XY stage. We are also planning to develop a product around this sensor – it is particularly attractive as a sensitive, robust, and inexpensive run-out sensor.

**THEORETICAL SRS SENSOR RESPONSE
FOCAL SPOT RADIUS AS A PARAMETER**

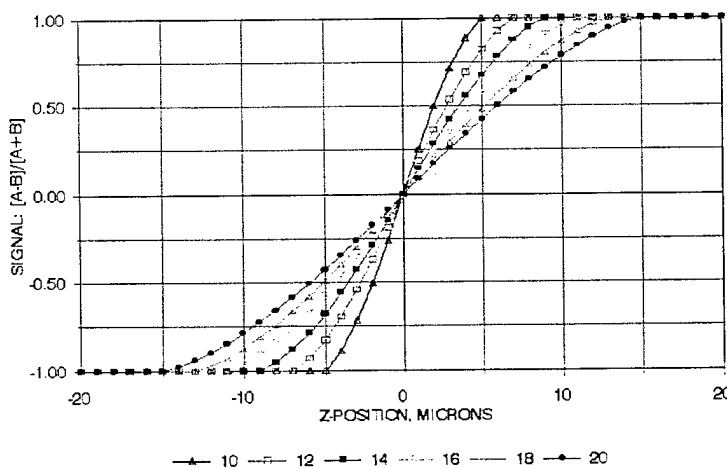


Figure 17A

These curves show the theoretical SRS sensor response to target surface displacement with the image spot radius as a parameter, and with a bi-cell gap of 8 microns. Based on ray-tracing the actual design, we can achieve a spot radius as small as 10 microns. For a 3 mwatt laser diode, we estimate that the shot-noise-limited target position resolution will be under 5 nm. (The numbers for the different plots are the radii of the laser spot diameters in microns. We can produce spots with $R \leq 10 \mu\text{m}$.)

NANOGAGE SENSOR CALIBRATION 4/17/98

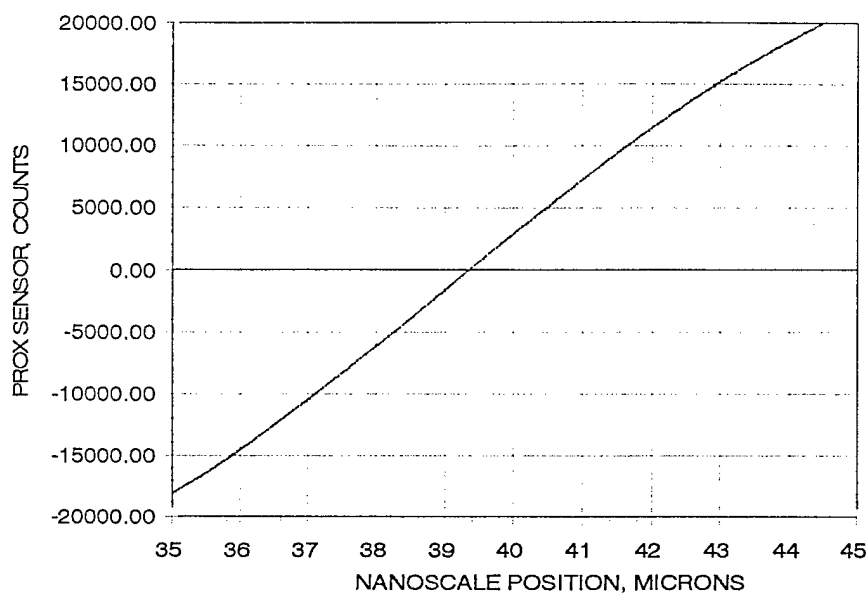


Figure 17B Experimental measurement of short-range sensor response

C.6 Demonstrate 2.5nm repeatability

There is a problem in demonstrating this specification using a laser interferometer which itself has a 5nm LSB and suffers from turbulence noise (rms value on the order of 10nm to 30nm).

To demonstrate repeatability with the XY Grid and sensor, we have elected to use two completely independent XY sensor heads (figure 18 shows the current sensor head), and to follow the following protocol:

1. Move the stage back and forth at nominally constant speed over a range on the order of 20mm.
2. Record the X and Y coordinates for both sensor heads, A and B;
3. Correct the data for velocity/latency errors; and
4. Assess the repeatability of the measured difference in positions recorded by sensors A and B.

This measurement — and any measurement of repeatability — depends on the assumed stability of the mechanical system (did the separation between the two sensor heads change? Did the stage rotate by a milliradian between the first and last measurements?): the sequence should be carried out quickly to minimize thermal effects and mechanical drifts. As described in section C.3, we have modified our stage design to accommodate a second sensor head; both sensor heads are attached to a massive Zerodur bar.

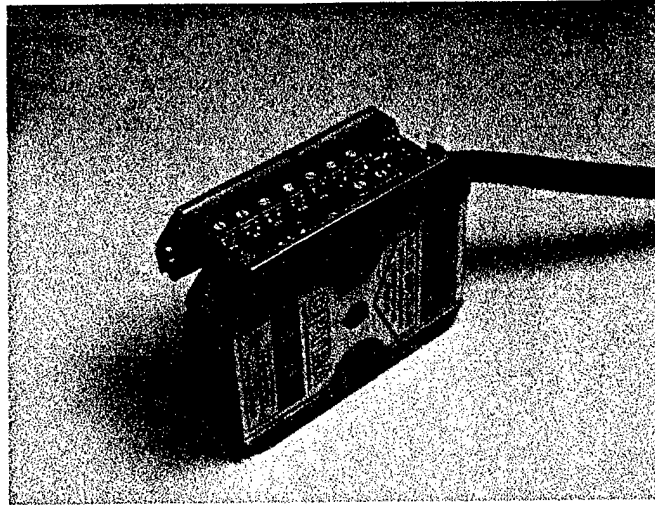


Figure 18 NanoGrid XY Sensor Head

Figure 19 shows the experimental results obtained in this manner. The stage was driven by a triangular waveform from a signal generator to traverse approximately 10 millimeters back and forth along the X-axis every 5 seconds. X position data for both sensor heads was recorded at 300 Hz, along with time. Figure 19A (top left) shows plots of the positions recorded by the two sensor heads, and of the difference between the readings from the two sensor heads (adjusted to have average values of zero). Figure 19B (top right) shows the position difference data and the stage velocity plotted as a function of stage position, and figure 19C (bottom left) shows the same data with a correction factor applied to correct for the time delay between the data readouts for the two sensor heads. This correction factor, equal to the mean differential data latency in microseconds, was set to its correct value by adjusting it to minimize the standard deviation of the position difference data. Based on these data the differential data latency had a value of 4.5 microsec. Figure 18D (lower right) shows an expanded portion of the data in figure 18C and suggests a standard deviation in repeated measurements of position at different locations of 1 to 2 nm.

At present, we can only speculate about causes for the errors in repeated position measurements. The most likely cause (in our present judgment) is variability in the differential data latency due to asynchronism in the three clocks that are involved in data collection (the clock in the data-collection computer, and the two clocks on the two XY sensor processor boards).

A scale calibration curve cannot be uniquely defined by the data from a pair of sensors, but the variations in the differential position measurements gives us a good idea of the non-linearities in the scale calibration curve: their peak-to-peak excursions, about 50 nanometers in this case, should be approximately equal. This value is consistent with other measurements of the scale non-linearity.

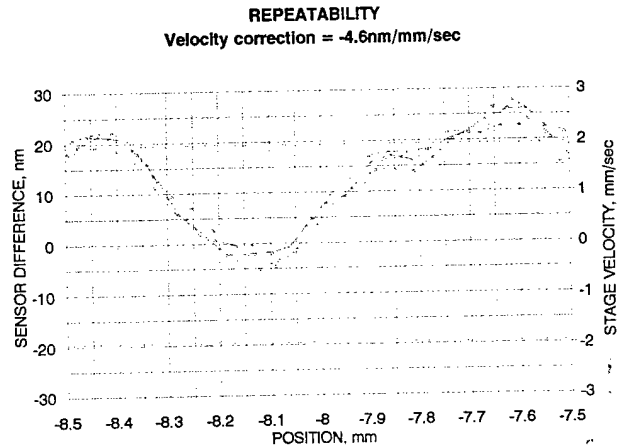
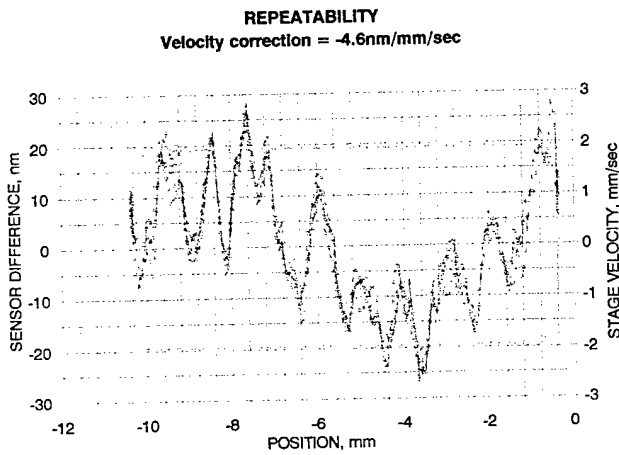
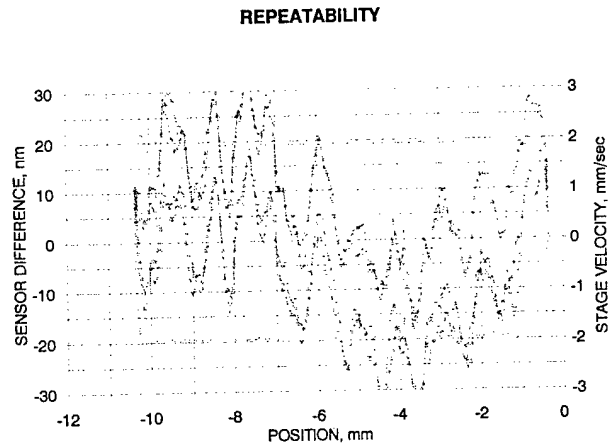
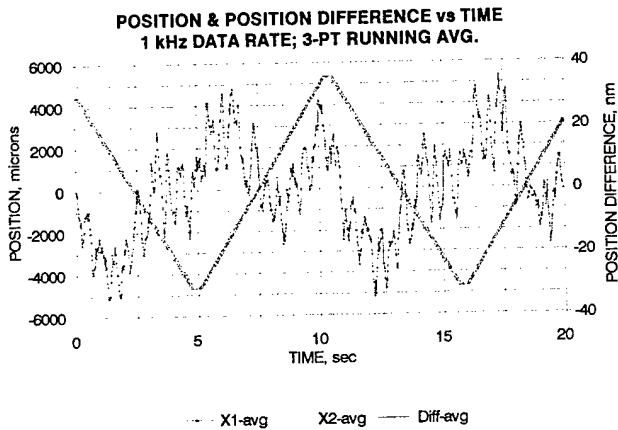


Figure 19 NanoGrid Repeatability Data

These plots are described in detail in the text; for all but figure 19A (upper left) the red curves are the differential position data, and the green curves are velocity data. All plots are based on the same set of data.

Figure 19A (upper left): plots of position recorded by each of two independent NanoGrid sensors (red and green), and a plot of the difference between them (blue) — all recorded as functions of time.

Figure 19B (upper right): plots of stage velocity (green) and differential position (red) as functions of stage position. Data is uncorrected for differential latency.

Figure 19C (lower left): same as 19B, only corrected for mean differential data latency of 4.5 microseconds.

Figure 19D (lower right): expanded portion of figure 19C showing a peak-to-peak repeatability on the order of 2 to 3 nanometers.

C.7 Demonstrate 1 m/sec velocity capability

We did not plan to modify the stage to operate at 1 m/sec during Phase I, but we did wish to show that the metrology sensor is capable of functioning at or close to a 1m/sec velocity. To do this, we used a radial encoder whose circumferential motion was sensed as an X displacement by the XY sensor head. This was a very convenient approach, since we didn't have to deal with the problem of accelerating a linear stage. We had a 45° radial encoder segment on hand with a radius of approximately 25mm. This was mounted on a variable speed spindle and rotated at increasing speeds until we began to see data errors due to the velocity. We recorded encoder position as a function of time, did a linear regression of the data against time, and then plotted the non-linearity of the position (i.e. the difference between the recorded data and the line from the linear regression) as a function of position. The curves in figure 20 are representative. The top curve, taken at a velocity of 192mm/sec, is smooth and well-behaved. The non-linearities are probably due to vibration of the rotating spindle assembly relative to the sensor head. In the lower plot, the velocity has been increased to 795mm/sec and we see the first signs of velocity-induced data degradation: the 2-point data drop-out is clearly an artifact, since there are no forces available to cause that type of acceleration and deceleration.

The top speed of ≈ 800 mm/sec is not unexpected for the current configuration. The speed of the NanoGrid is limited by the unwrapping circuit that counts integral cycles of phase. The circuit detects phase discontinuities by comparing successive phase measurements. When a discontinuity of $\frac{1}{2}$ cycle or greater is detected, the position counter is incremented or decremented. If the phase changes by more than $\frac{7}{16}$ cycle between measurements, the position counter will mis-count, and position measurement will be lost.

The existing design measures phase at a 750kHz rate for 2 axes, or 375kHz per axis. Maximum speed is $(7/16) \times 375 \times 10^6$ cycle/sec $\times 5 \times 10^{-6}$ meter/cycle ≈ 820 mm/sec.

Increasing the phase measurement update rate can increase the maximum speed. A 2x increase can be achieved by eliminating the multiplexing. Also, faster A/D converters will increase the maximum speed. Using multiplexing, to achieve 1 meter/sec, the update rate must be > 915 KHz. 12 bit A/D converters with update rates of > 1 MHz are available. We are confident that we will be able to handle speeds of at least 1 meter/sec during Phase II.

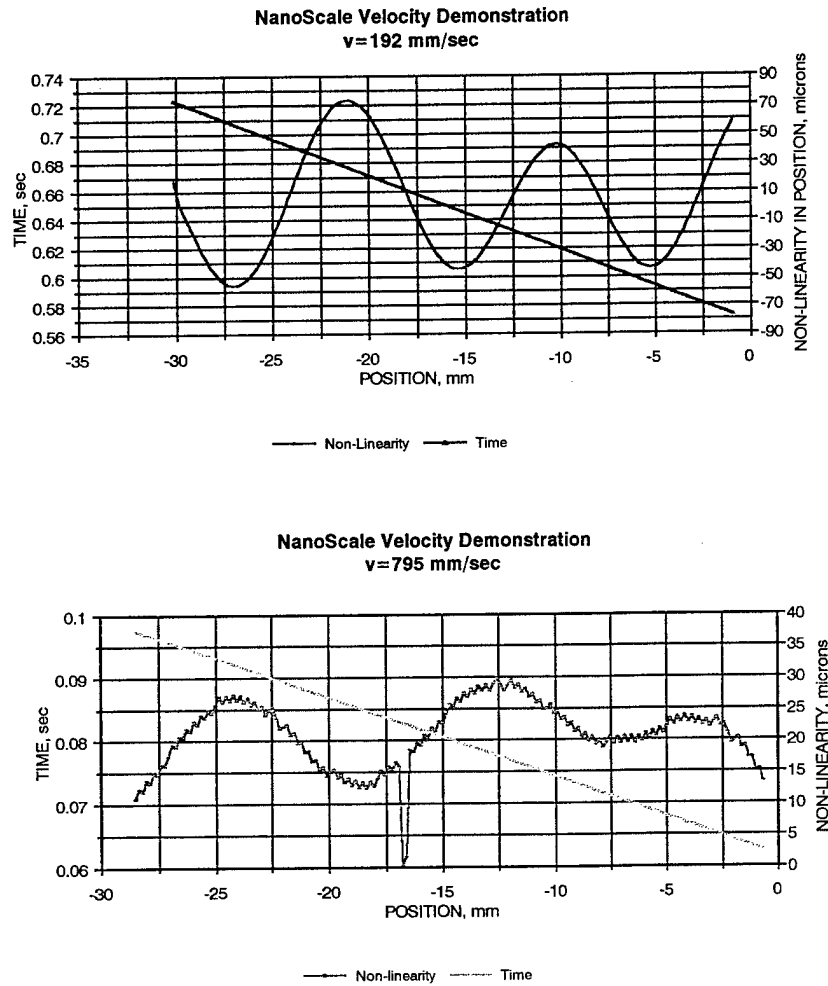


Figure 20 Onset of Velocity Errors at 795mm/sec

The top plot shows position data being collected without difficulty at a linear speed of 192mm/sec.

The bottom plot shows the first signs of data degradation at a speed of 795mm/sec. This current limitation is due to the maximum data rate of 375 kHz (multiplexed) which is set by the speed of the A/D's used in our phase processor board. We can reach a velocity of 1 m/sec either by eliminating the multiplexing, or by switching to fasted (1 MHz) 12-bit A/D converters.

C.8 Resolution / Noise Measurement

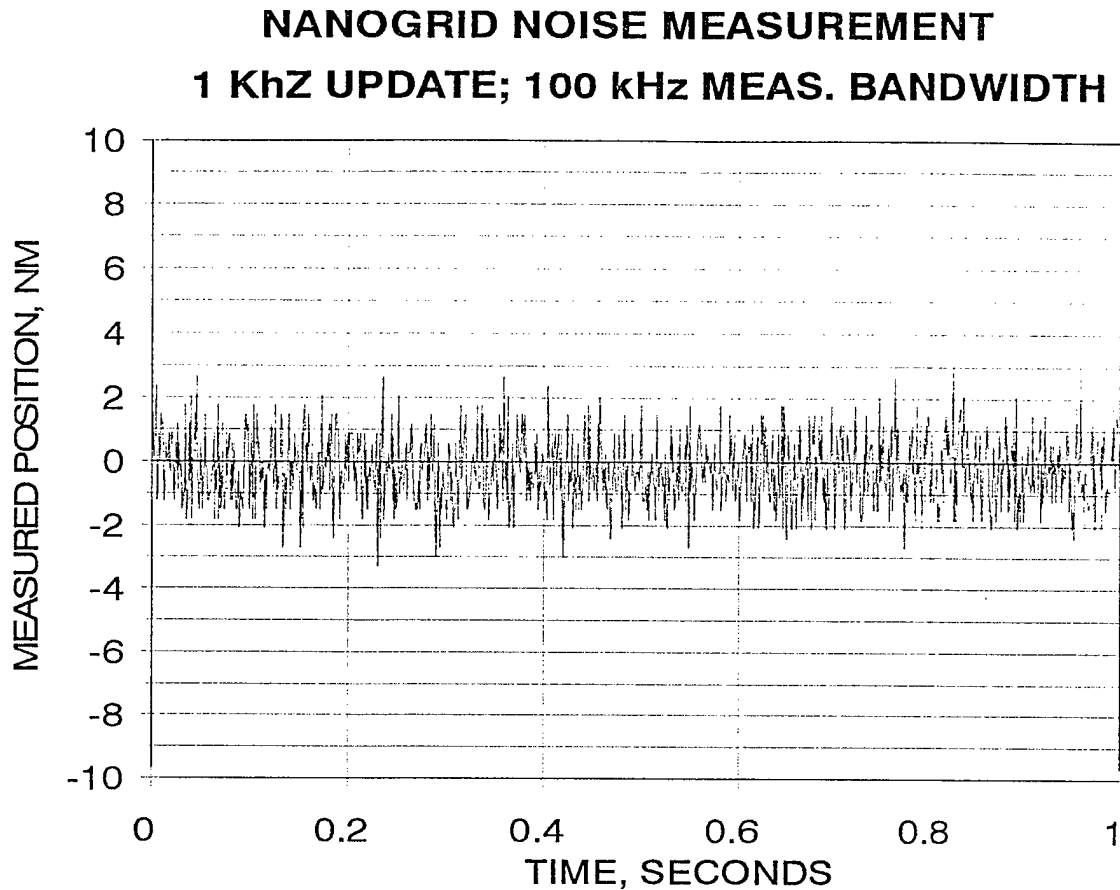


Figure 21 Resolution / Noise Measurement

This figure shows a plot of the output from one axis of the NanoGrid sensor with the XY grid nominally at rest (clamped in a quiet room). The data was collected at 1 kHz, but the measurement bandwidth was $\approx 100\text{kHz}$. A Fourier analysis showed that the noise was essentially white, with a spike at DC.

Measurement resolution is limited either by digitization or noise, and is a function of measurement bandwidth. In this instance, the LSB is 0.3nm (the 5000nm effective grid interval divided by 2^{14} , where we have a 14-bit phase signal) and for measurement bandwidths of practical interest, the resolution is close to shot-noise-limited. Figure 21 above shows the recorded NanoGrid position signal for a clamped (stationary) stage. The standard deviation (Noise-equivalent-displacement, $\text{NE}\Delta x$) in this signal is 1.05 nm , which is roughly $2\times$ the calculated shot-noise-limited value of $\text{NE}\Delta x$ for a 100kHz measurement bandwidth. $2\times$ isn't bad for a complex radiometric calculation involving multiple detectors, preamps, and phase processors, and we feel that in terms of radiometry and noise the system is performing satisfactorily. In the future we will be increasing the power at the detector, both by increased output from the laser diode

source and improved grating efficiency at the encoder, and should be able to bring the shot noise down to the level of an LSB.

C.9 Evaluation of XY Grid made on an Etec ALTA machine

As described earlier, laser-interferometer-controlled step-and-repeat lithography cameras are not adequate for the fabrication of accurate XY grids for metrology. The Etec CORE machine was found to be excellent for fabricating grids up to between 6 and 7-inches on a side, and it was our plan to use an Etec ALTA machine (capable of direct-writing over a square area of about 8.4-inches on a side) to make an 8-inch XY grid for evaluation. As described in section C.1, we have been working with Photronics extensively to that end, and had ordered an 8-inch grid from them for delivery in May, 1998. In fact, Photronics worked hard to achieve our objective, but was unable to do so.

9-inch quartz plates were (and are) very difficult to get hold of, but we were successful in purchasing a pair for coating and exposure by Photronics. There was a delay while Photronics added the capability to handle 9-inch square plates to their ALTA machine, and finally in late May they made a test exposure on a 6-inch plate and then attempted to expose and then process our 9-inch plate. The procedure was complicated by the fact that the ALTA machine was in San Jose and the automated processing equipment for 9-inch plates was in Colorado Springs – and the latent exposure had a lifetime on the order of 8-hours. So the plates had to be exposed, shipped by air to Colorado Springs, and processed within 8 hours. For whatever reason, when the 8-inch plate was exposed and processed, the grid pattern was barely visible, and was certainly too weak for use as an XY encoder. During the next exposure attempt, the 9-inch plate-loading mechanism for the ALTA machine was damaged, and subsequent repair attempts by Etec and Photronics were unsuccessful.

By this time the ALTA machine, which is profitably used by Photronics for the volume production of very high quality 6-inch masks, had been taken away from that task for more than two weeks. Photronics was unable to make it available to us for any longer, and the attempt to make an 8-inch grid on a 9-inch plate was abandoned. We do, however, have a portion of the 6-inch plate that had been used to check the exposure, and have tested it to validate the accuracy of the ALTA machine. The results are shown in figure 24. In scans over approximately 50mm, the grids appear to be excellent, with an average peak-to-peak non-linearity of 84 nm. The error curves had no noticeable high spatial frequencies. Clearly, the ALTA machine is well-suited to our needs. Photronics plans to solve the problems with 9-inch plates (their own production schedule calls for the manufacture of 8-inch reticles on ALTA machines), and we may be more successful in getting an 8-inch grid from Photronics at some time in the near future.

In the meantime, we have been exploring the use of a Micronic (Micronic Laser Systems, Täby, Sweden; www.micronic.se) LRS 200 Laser Writer lithography system. Micronic Laser Systems offer the exciting capability of going to 13-inch plates with specifications comparable to those of the Etec ALTA machine. We have ordered a 6-inch test plate from Image Technology Inc. (Palo Alto, CA; www.image-tec.com), who just acquired a Micronics LRS200 machine capable of writing plates up to 9-inches in size. We may have

ALTA GRID CALIBRATION: 6/15/98

3" x 3" Section of 6" Quartz Plate

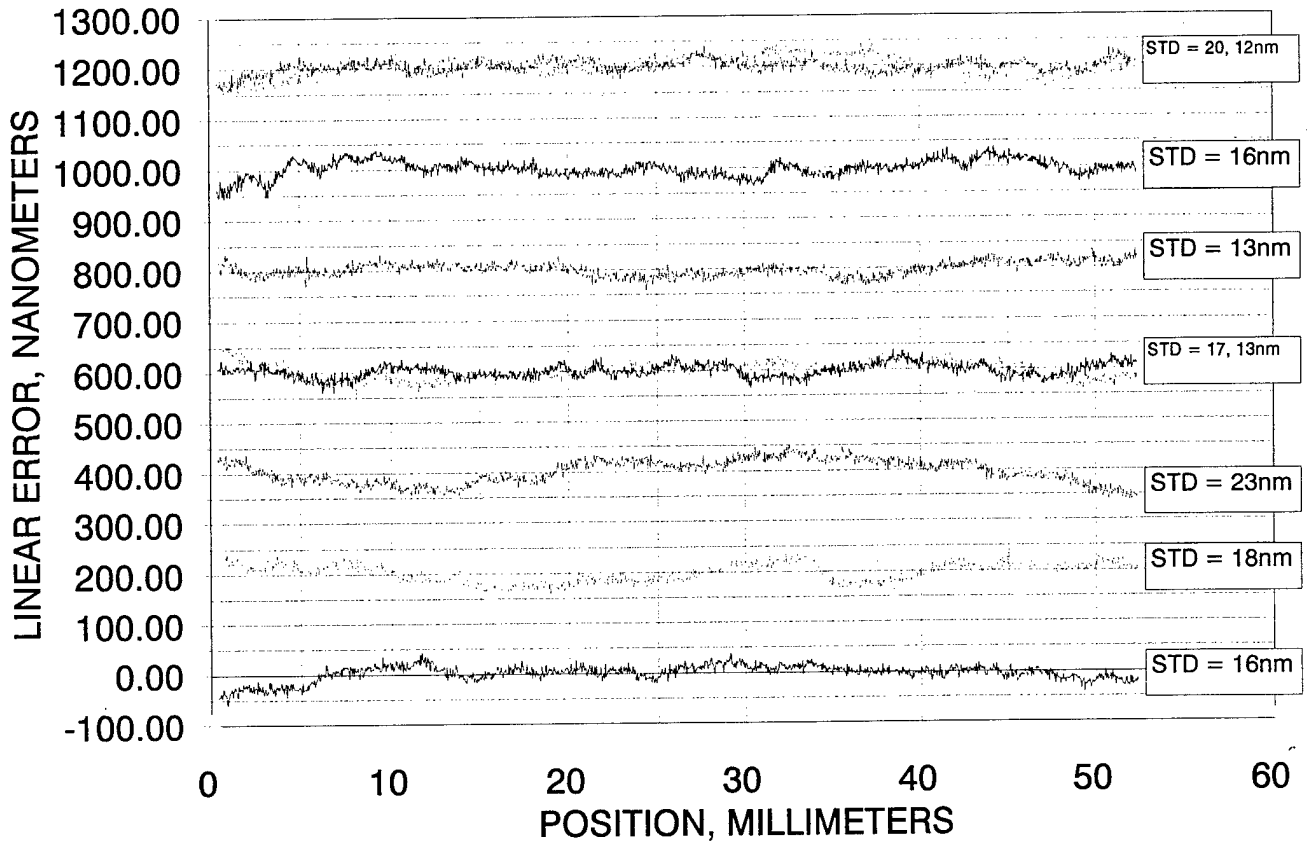


Figure 24 Grid made on Etec ALTA Laser Writer

These are the best data we have seen from any microlithography machine. The high-spatial-frequency content is extremely small (on the order of 10nm in amplitude) and the overall accuracy is excellent (STD's in the range of 10nm to 20nm; peak-to-peak \approx 100 nm). Most of what appears to be low-spatial-frequency is probably due to turbulence in the laser interferometer (note that it is not repeatable in the pairs of duplicate runs at the top and center of the graph).

Based on what we have seen to date, the ALTA is the machine of choice for making grids.

IMAGE TECH. LRS200 GRID CAL.: 6/16/98
Scans 11.43mm apart; offset by 200nm

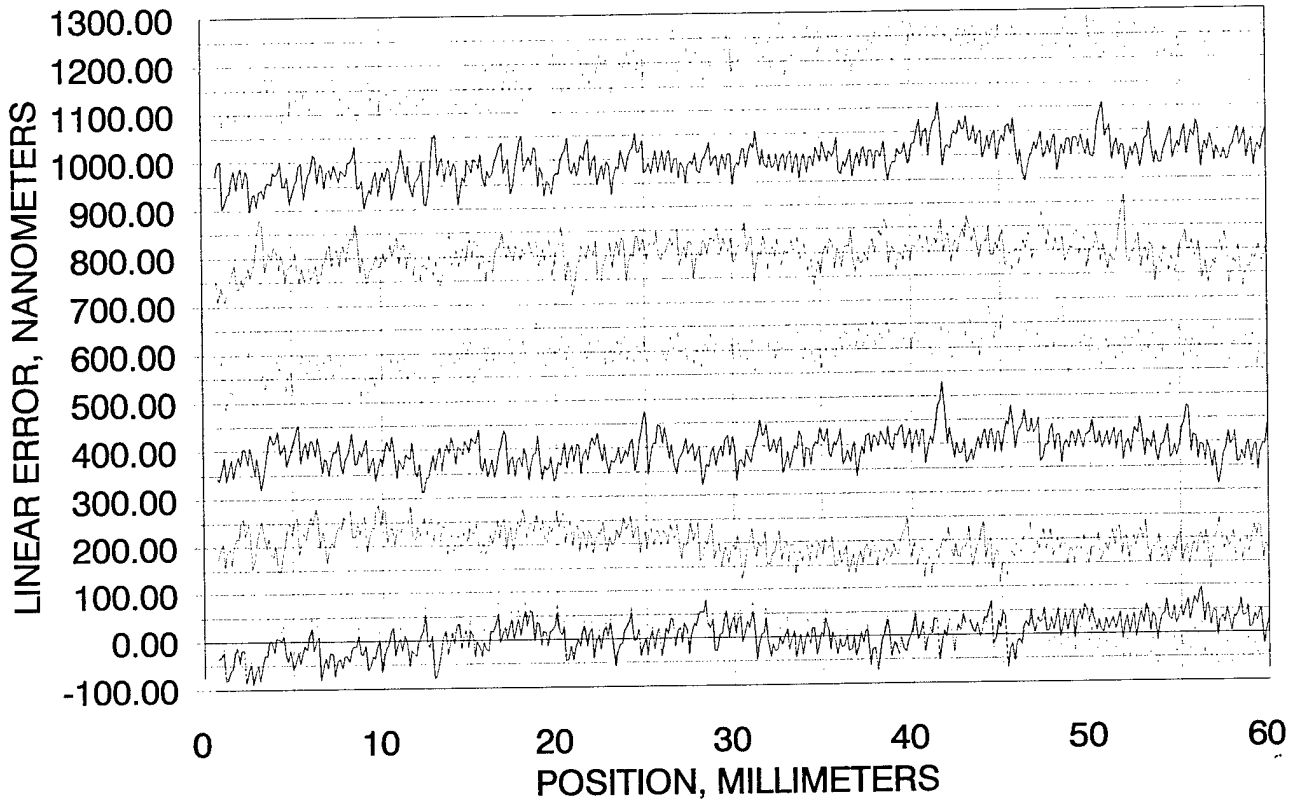


Figure 25 Grid made on a Micronic LS200 Laser Writer

This is one of the first products of a new LS200 machine recently acquired by Image Technology, Inc. The overall accuracy is excellent (very straight plots), but there is a large-amplitude high-spatial-frequency component to the calibration curve. The average STD and peak-to-peak values for these data are 36nm and 215nm respectively. Since this machine has just been installed, it may well improve in performance as it is more finely tuned and stabilized.

this plate in time to include accuracy data in this report. In any event, if the test plate meets our specifications, we will be in a position to have one of our 9-inch quartz plates written and processed very early in a Phase II program.

Note: As this report was in the final editing stage we did receive the grid made by Image Technology Inc. using a Micronic LS200 machine. The initial calibration data are shown in figure 25 (previous page). As noted in the caption, the grid has a high overall accuracy, but has relatively large-amplitude high-spatial-frequency components. This may well improve with time as Image Technology becomes more experienced with the use of the LS200, and as it is more finely tuned.

Figure 26 below provides an interesting comparison between the three best laser-writer machines we have seen to date: the ALTA 3000, the CORE (both manufactured by Etec), and the Micronics LS200. They are all far better than step-and-repeat cameras, and of the three the ALTA machine is superior by a clear margin.

LRS200 vs. CORE vs. ALTA 3000: 6/16/98

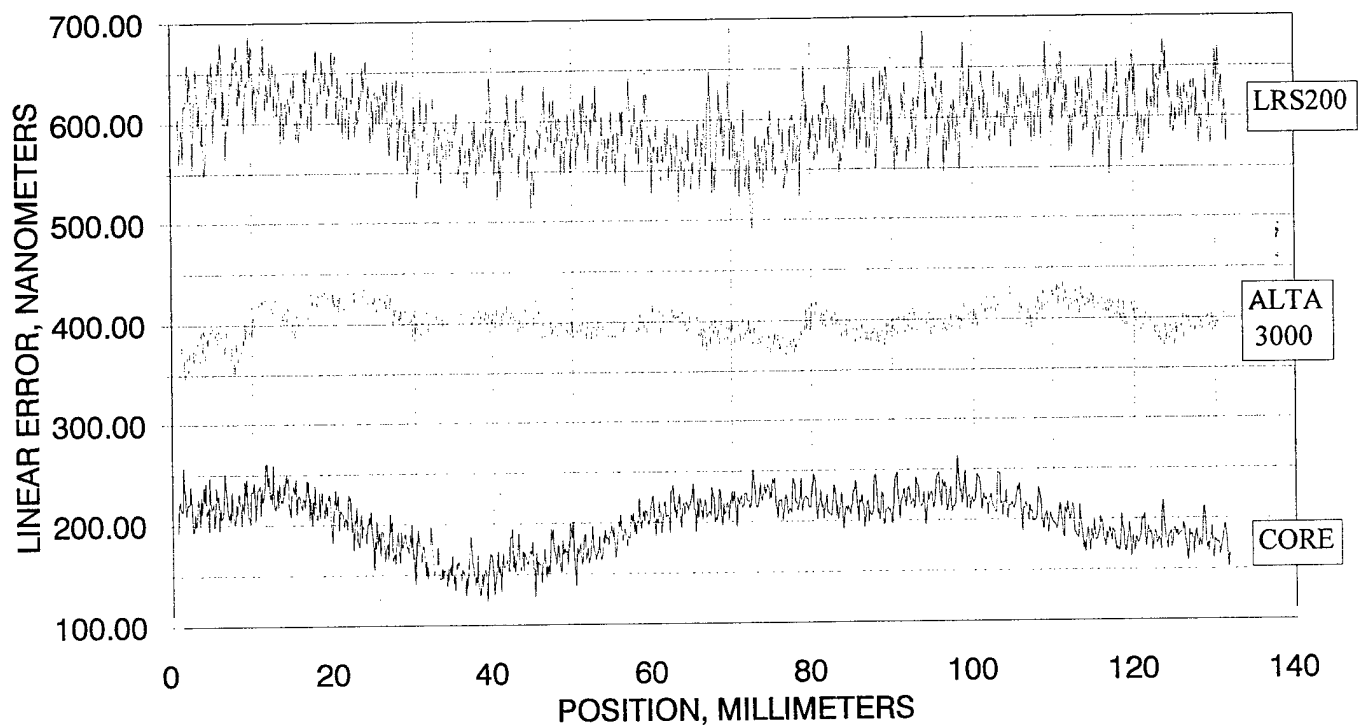


Figure 26 Comparison of grids made on ALTA, CORE and LS200 machines

(Noisy lab, as evidenced by turbulence effects)

D. Report on NanoGrid marketing and sales.

The long-term goal of this SBIR program is the development of new technology to help semiconductor manufacturers continue to increase component density on chips, and to utilize larger wafers. Our particular focus is on the realization of a metrology technology that will allow better positioning repeatability and the use of higher stage speeds. We have already developed a NanoGrid sensor head and associated electronics for use with XY grids having a 10 μ m physical pitch (5 μ m metrology pitch), and are presently able to supply grids up to 150mm \times 150mm (these products are described on our web site, www.optra.com).

Although our ultimate target market is the semiconductor lithography business, our initial sales have been to customers in the wafer and mask inspection and repair business, where their concerns are vacuum compatibility, sub-micron accuracy and repeatability, and the capability to upgrade to 200mm and 300mm grid sizes.

Manufacturers of semiconductor lithography machines are conservative when it comes to metrology (hardly surprising!), and — even though they know they are pushing the limits of interferometer-based metrology — reluctant to change the concept of their stage and metrology configuration. The ideal (in our judgment) stage/metrology configuration — consistent with the current notion of a relatively massive moving stage which supports the wafer or reticle — is shown in figure 27. Its key features are:

- The XY grid and the wafer are coplanar, to eliminate Abbe errors in Z;
- The sensor head is rigidly attached to the lens mount and the XY grid is rigidly attached to the moving stage;
- The overall system is compact — far more so than a laser-interferometer system.
- A single-axis sensor is added to the XY sensor to allow measurement of rotation about the Z-axis.

This configuration is markedly different from the conventional laser-interferometer stage (figure 28), and its adaptation has to occur early in the design cycle to allow for its intelligent integration into the total lithography system. Our marketing plan is to establish the reliability and high performance of the XY Grid approach to metrology in secondary market areas, and then to aggressively approach customers in the lithography market. The capabilities that we add during the course of this SBIR program — increased accuracy and repeatability, high-speed, and 300mm coverage — will serve us very well in bringing this technology to the semiconductor lithography market.

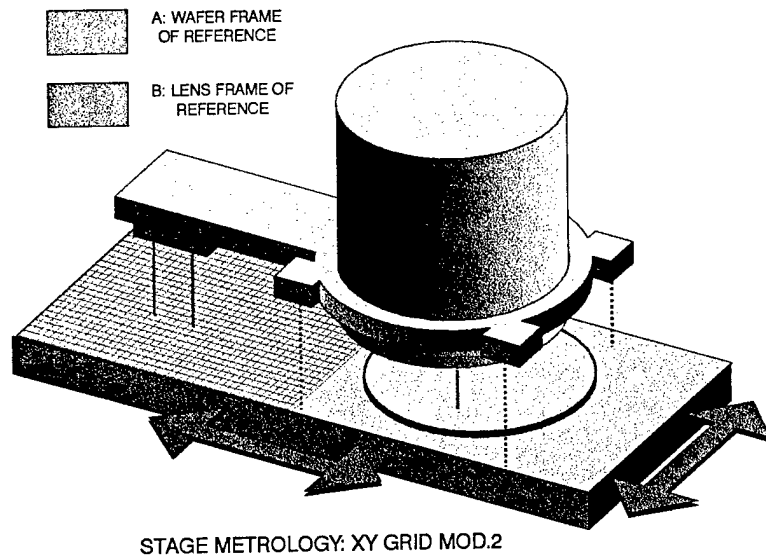


Figure 27 NanoGrid Lithography

The XY grid is on the stage next to the wafer; the sensor heads (XY and X') are attached to the lens housing and to the left of it. The 3 sensors around the lens are short-range sensors that monitor the level of the stage relative to the lens. The metrology goal is to monitor the position of the red components relative to the blue components.

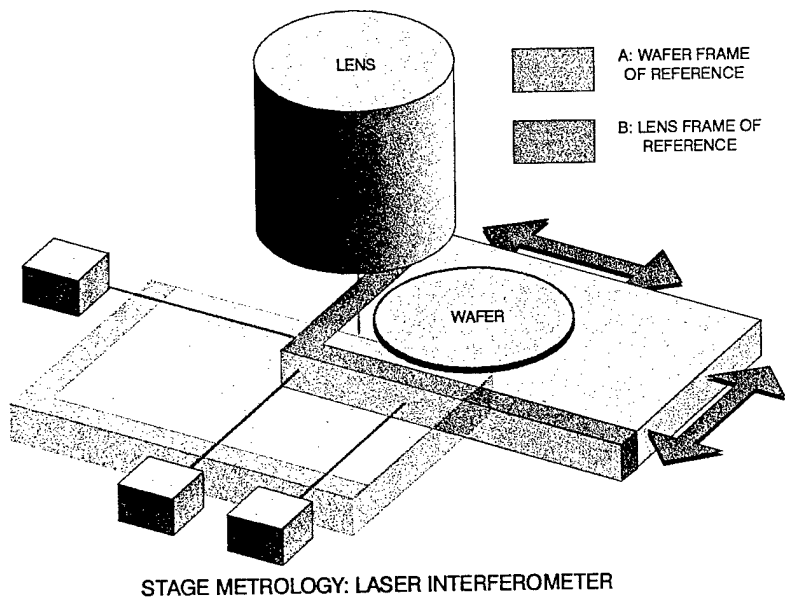


Figure 28 Interferometer Stage

The three small blue boxes are the interferometers for monitoring X, Y and θ_z , and the green rectangle shows the stage location at one extreme of its range of motion. One of the mechanical problems of this arrangement is that of rigidly maintaining the position of the interferometers relative to the lens; another is the problem of turbulence along the optical paths — which can be twice as long as the displacement range of the stage. As pointed out in the text, the cost of the L-shaped interferometer mirror exceeds that of the XY grid by a substantial margin.